Quantum Astronomy

Cesare Barbieri
Emeritus of Astronomy
University of Padova

Main collaborators:
Giampiero Naletto (DEI, DFA)
Luca Zampieri and Massimo Calvani (INAF OAPd)
Andrej Čadež (University of Ljubliana)
Roberto Mignani (CNR)
Mauro Barbieri (University Chile)
Gabriele Rodeghiero (MPI Heidelberg)
Andrea Richichi (ESO and NARIT)

All of Astronomy in Time and Frequency

This slide conveys the idea of all of Astronomy in a time – frequency domain, and of the *lower limit imposed by Heisenberg principle*.

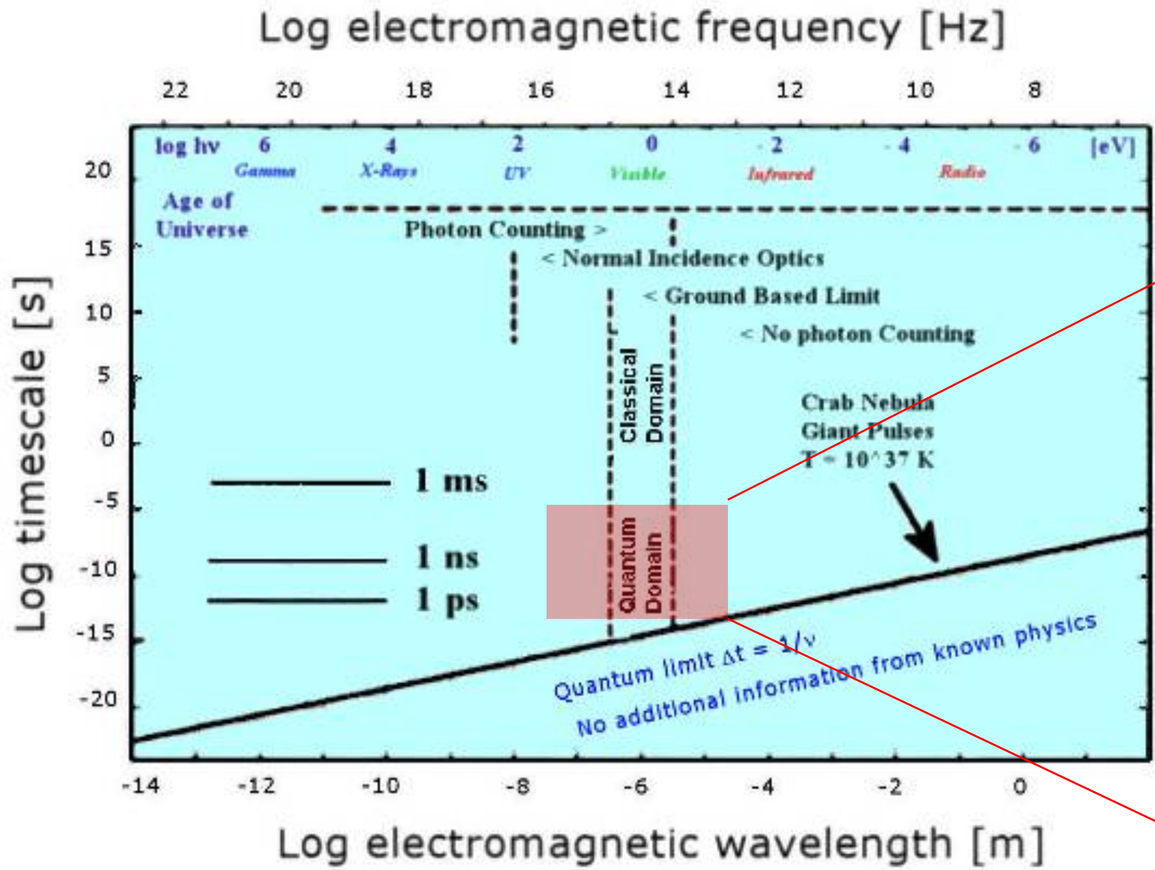

L3 CCDs
MCP
STJ
TES
PM
SiPM
HPD
APD
SPAD
SSPD
…

Pushing the time resolution *towards the limits imposed by Heisenberg's principle* might have the same scientific impact of opening a new window. This new Astronomy can be designated as *Quantum Astronomy, or Photonics Astronomy*.

Some thoughts on quantum optics and astronomy

Photons are very complex entities, carrying more information than extracted in astronomical applications with conventional techniques of imaging, spectroscopy and polarimetry.

An important breakthrough occurred with the invention of the ***laser.*** According to Glauber, Arecchi, Mandel, etc. seminal papers (from 1963 onwards), arbitrary states of light can be specified as first, second, and higher order ***correlation functions*** **$G^{(1)}$, $G^{(2)}$, …,** with respect to position ***r*** and time *t*.

Properties of the photon stream

Such properties are ***reflected in the second- (and higher) order coherence of light*** . Therefore, one has to investigate the ***correlation in time or space between successive photons*** in the arriving light beam.

Realistically, in astronomical applications we hope to detect **second-order correlation effects,** which can be ascribed to quantities of type ***I *I*,** i.e. intensity multiplied by itself,

Second Order Correlation Function

$$g^{(2)}(d,\tau) = \frac{\langle I(\mathbf{r}_1,t_1) I(\mathbf{r}_2,t_2)\rangle}{\langle I(\mathbf{r}_1,t_1)\rangle\langle I(\mathbf{r}_2,t_2)\rangle}$$

(R. Glauber, 1965, Nobel Prize 2005)

with $\mathbf{r_2}$-$\mathbf{r_1}$=$\boldsymbol{d}$ and t_2-t_1=τ

1. If $\tau = 0$ and $\boldsymbol{d} \neq 0$ one gets Hanbury Brown - Twiss **Intensity Interferometry**, in the following called also **Stellar II**, **SII,** which will be discussed later on
2. If $\tau \neq 0$ and $\boldsymbol{d} = 0$ one gets **photon correlation spectroscopy**, capable to achieve spectral resolutions R $\approx 10^9$- 10^{10}, necessary to resolve ***lased*** spectral lines, which will not be discussed further, although there might be astronomical applications.

Our first study:
QUANTEYE
for the
European Southern Observatory
(ESO)

OWL Instrument Concept Study

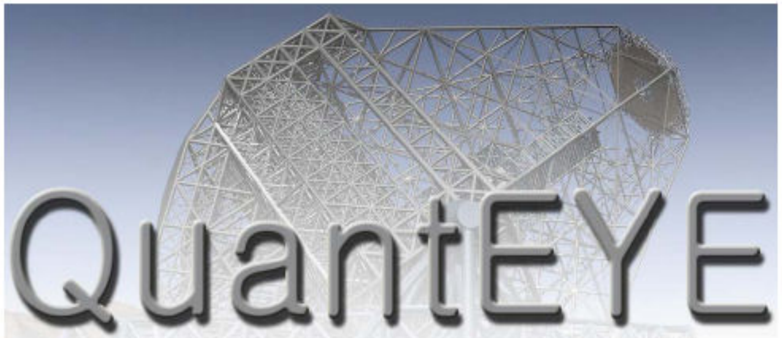

QUANTUM OPTICS INSTRUMENTATION FOR ASTRONOMY

D. Dravins[1], C. Barbieri[2],
V. Da Deppo[3], D. Faria[1], S. Fornasier[2],
R. A. E. Fosbury[4], L. Lindegren[1], G. Naletto[3], R. Nilsson[1],
T. Occhipinti[3], F. Tamburini[2], H. Uthas[1], L. Zampieri[5]

(1) Lund Observatory, Box 43, SE-22100 Lund, Sweden
(2) Department of Astronomy, University of Padova, Vicolo dell'Osservatorio 2, IT-35122 Padova, Italy
(3) Dept. of Information Engineering, University of Padova, Via Gradenigo, 6/B, IT-35131 Padova, Italy
(4) Space Telescope-European Coordinating Facility & European Southern Observatory, Karl-Schwarzschild-Straße 2, DE-85748 Garching bei München, Germany
(5) INAF – Astronomical Observatory of Padova, Vicolo dell'Osservatorio 5, IT-35122 Padova, Italy

LUND UNIVERSITY

OWL-CSR-ESO-00000-0162

Those concepts were exposed in our study *QuantEYE* (the ESO Quantum Eye, 2005) in the frame of the studies for the 100m Overwhelmingly Large (OWL) telescope.

The study had two main goals:

- Summarize the features of quantum optics applicable to Astronomy on a very large aperture

- demonstrate the feasibility of an instrument capable to reach the **picosecond time resolution** needed to bring quantum optics concepts into the astronomical domain

From OWL to ELT

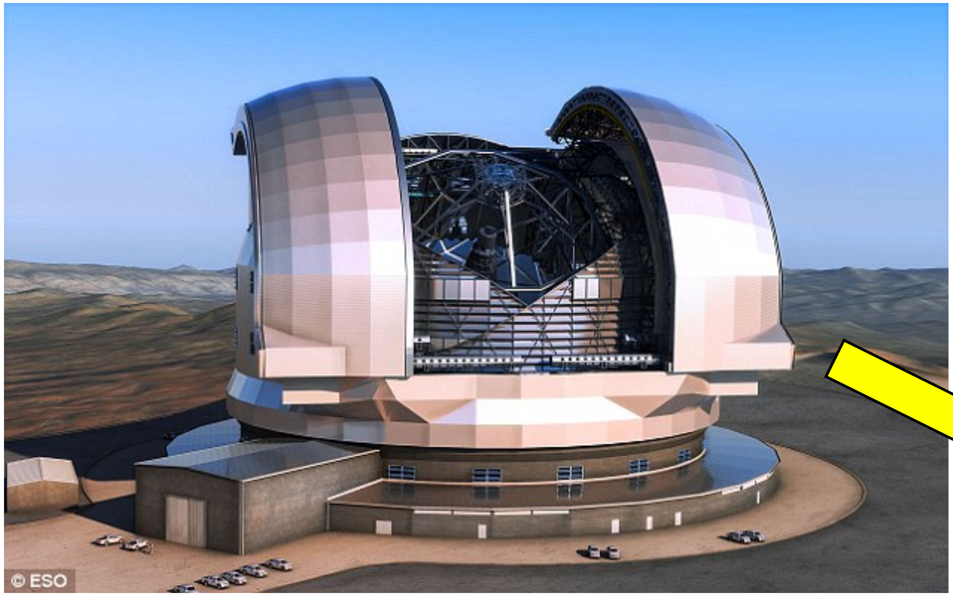

Few years after the completion of Quanteye, the telescope was downsized from 100m to 39m and renamed ELT, but still many concepts maintain their full validity.

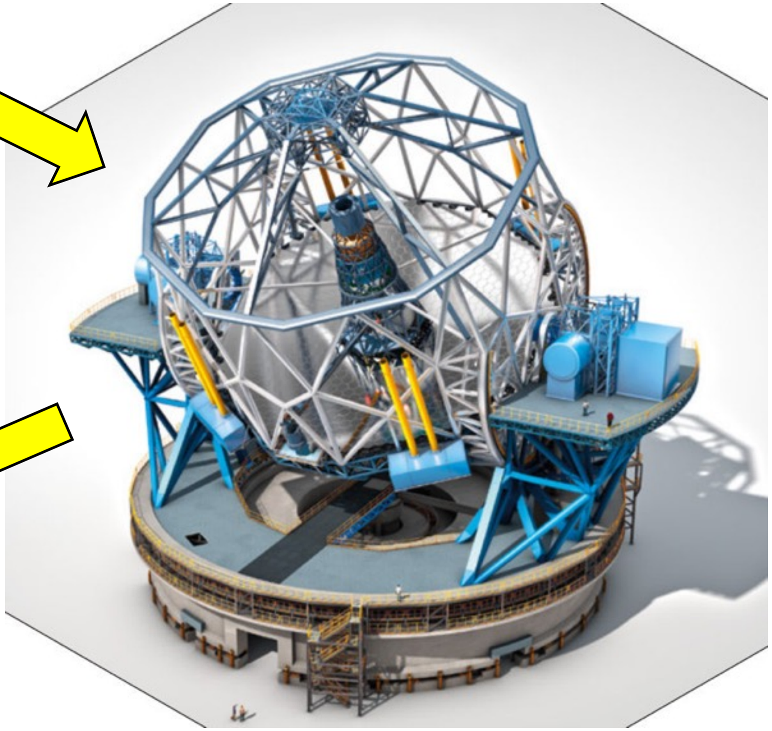

Cerro Armazones, the E-ELT site

Astrophysics below the millisecond

In addition to quantum effects, below the millisecond frontier there are more conventional astrophysical phenomena, e.g.:

Earth Atmospheric phenomena
<u>Lunar occultations*</u>
<u>Diameters and surface structures of stars*</u>
<u>Structures in the atmospheres of exoplanets*</u>
Surface convection on white dwarfs
<u>Neutron stars, optical pulsars (see later)*</u>
Photon bubbles in accretion flows
<u>Variability near X-ray binaries, black holes*</u>
Free-electron lasers around *magnetars*

......

and then ***the unexpected***…

* **<u>Already carried on in Asiago</u>**

From theory to reality: the key technological limitation is the detector

The most critical point, and driver for the design of QUANTEYE, was the selection of very fast, efficient and accurate ***photon counting detectors***.

No detector on the market had all needed capabilities: in order to proceed, we choose ***SPADs (Single Photon Avalanche Diode Detectors) operating in Geiger mode***, and produced by ***MPD*** in Bolzano (Italy).

The main drawbacks of those SPADs were the **small dimensions** (50 - 200 μm), **the lack of CCD-like arrays**, the **70 ns dead-time** and the **1.5% after-pulsing probability**.

To overcome both the SPAD limitations and the optical difficulty of coupling the pupil of a large telescope to very small detectors, we ***split*** the large telescope pupil into **10×10 sub-pupils**, each of them focused on a single SPAD, giving a total of ***100 distributed*** SPAD's.

In such a way, a “sparse” SPAD array ***collecting all light and coping with very high count rate*** could be obtained. The distributes array samples the telescope pupil, so that a system of ***100* parallel smaller** telescopes was realized, ***each one acting as a fast photometer.***

QuantEYE for OWL optical design

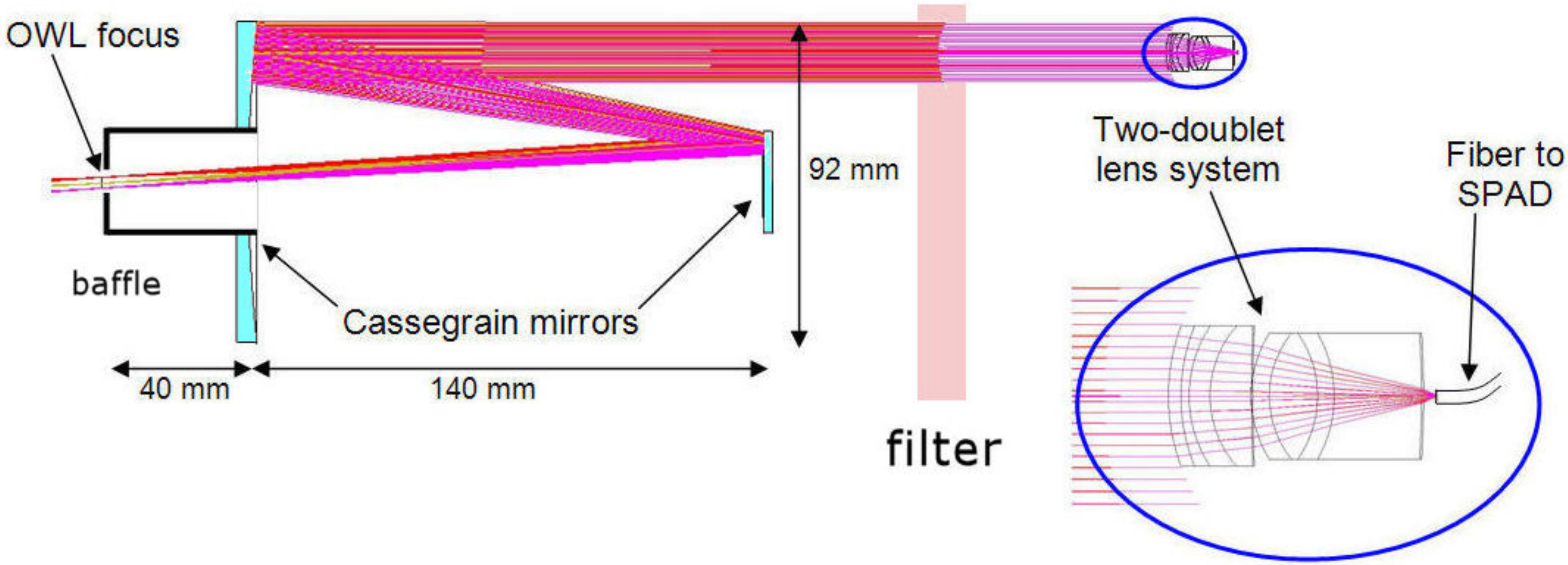

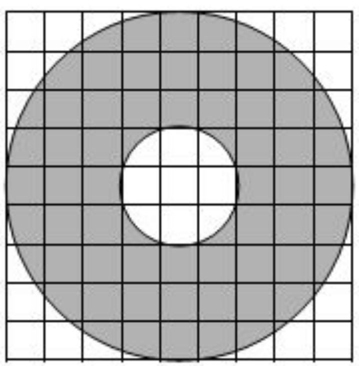

telescope pupil
subdivision

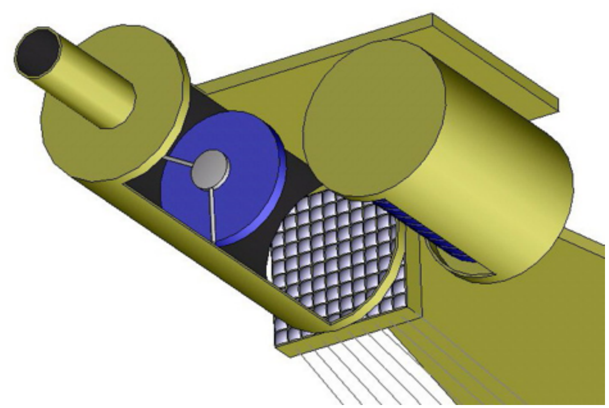

Advantages of this optical design

- Feasible optical design
- Count rate increased by N^2 with respect to the maximum count rate of a single SPAD. In the assumption $N = 10$ (100 SPAD's), the global count rate becomes 1 GHz (one photon every 100 ns on each SPAD);
- Detector redundancy;
- By cross-correlating the N^2 counts, a digital Intensity Interferometer is realized among the N^2 different sub-apertures, across the full telescope pupil.

Overall QuantEYE block diagram

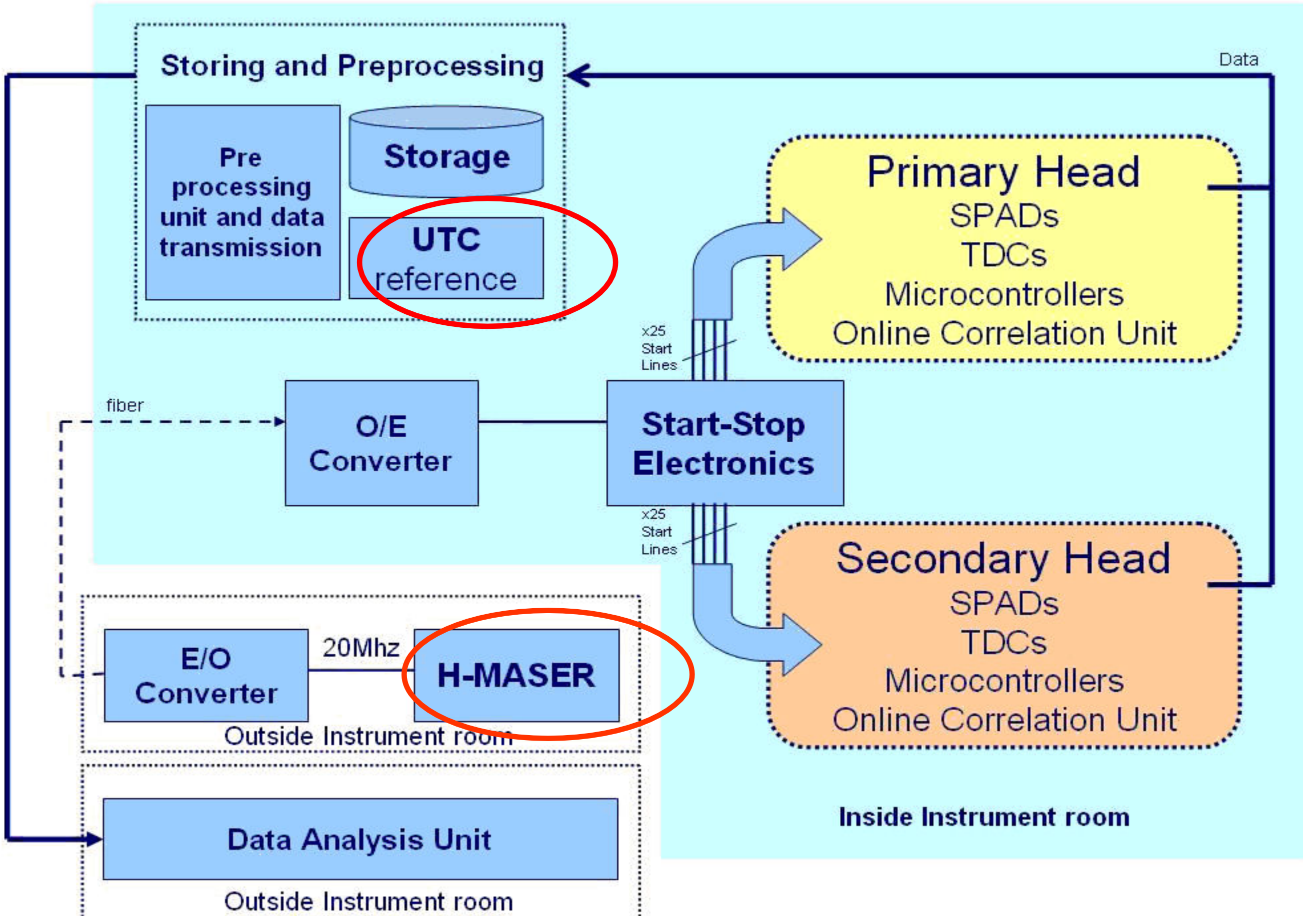

The overall system: two heads (one for the scientific target, the second one for a reference star), controls, storage, **time unit**.

Regarding time, please remember that in astronomy a **continuous time, common** to all ground and space telescopes is needed, and that data must be referred to a common origin, e.g. **the barycentre of the Solar System**.

From the design to the realization of prototypes: Aqueye and Iqueye

To gain real experience with those novel instrumental concepts, we designed and built two prototypes for much smaller telescopes:

Aqueye, for the 1.8m Copernicus telescope in Asiago - Ekar,

Iqueye, for a 4m class telescope (initially the ESO 3.5m NTT in La Silla, then the TNG and WHT in La Palma (now back in Asiago-Pennar, at the 1.2m Galileo telescope).

Aqueye and Iqueye were, and still are, the best time machines available to Astronomy, so that even with relatively small telescopes, we carry out frontier scientific observations, thanks to the **very accurate timing stamp capabilities, high efficiency and very large dynamic range of the photometers**.

Aqueye and Iqueye optomechanical design

The light beam is divided in ***four parts*** by means of a pyramidal mirror. Each beam is then focused on its own SPAD by a 1:3 focal reducer made of a pair of doublets.

Different filters can be inserted in each arm.

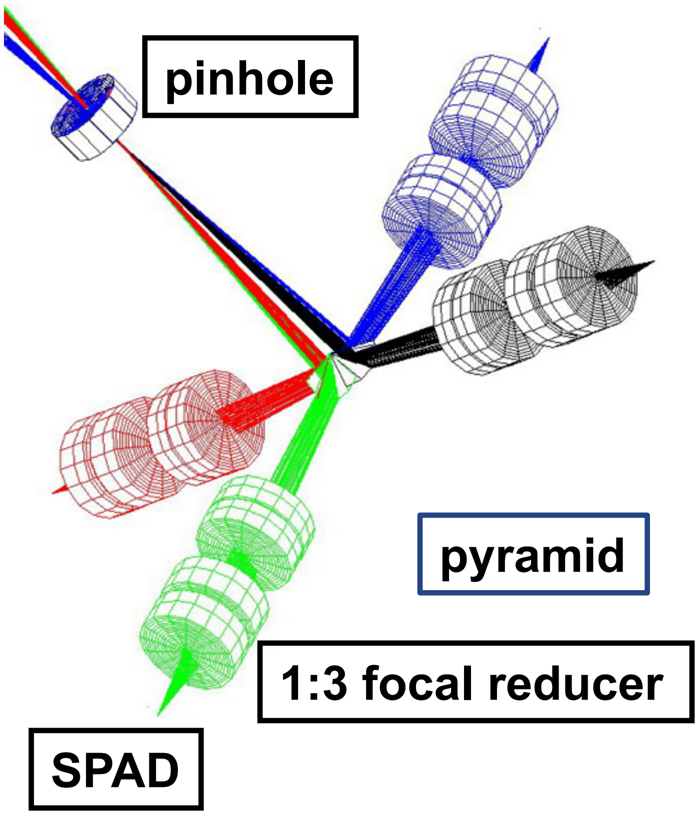

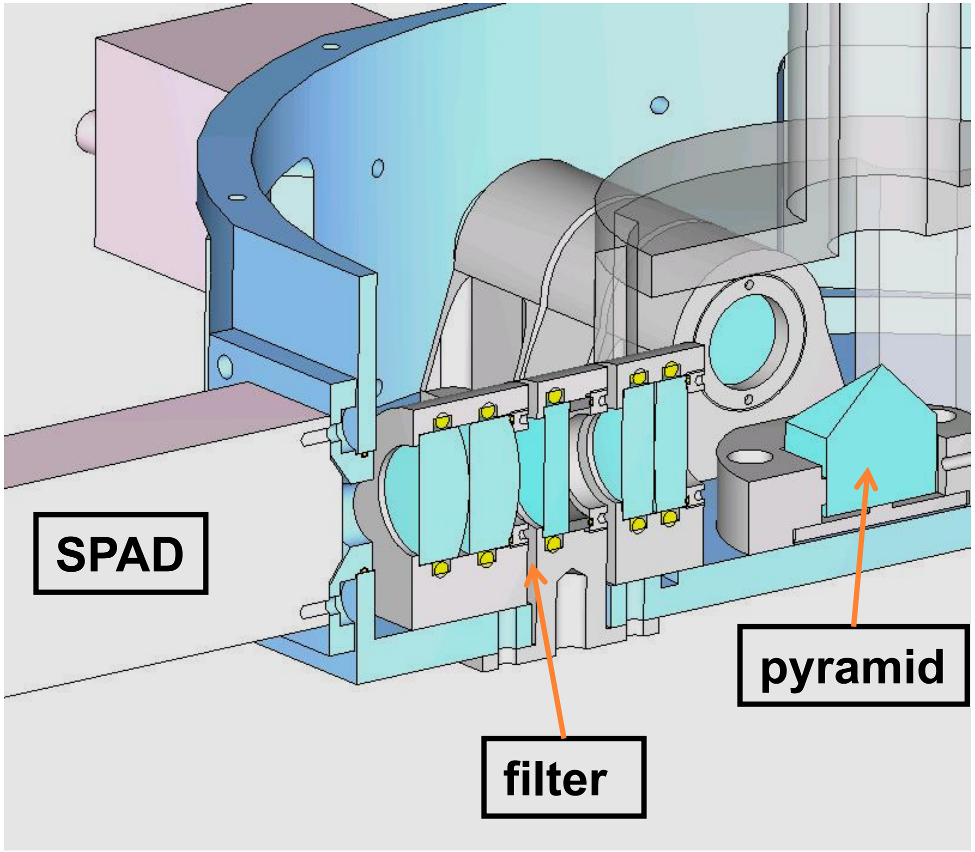

Aqueye Optomechanics

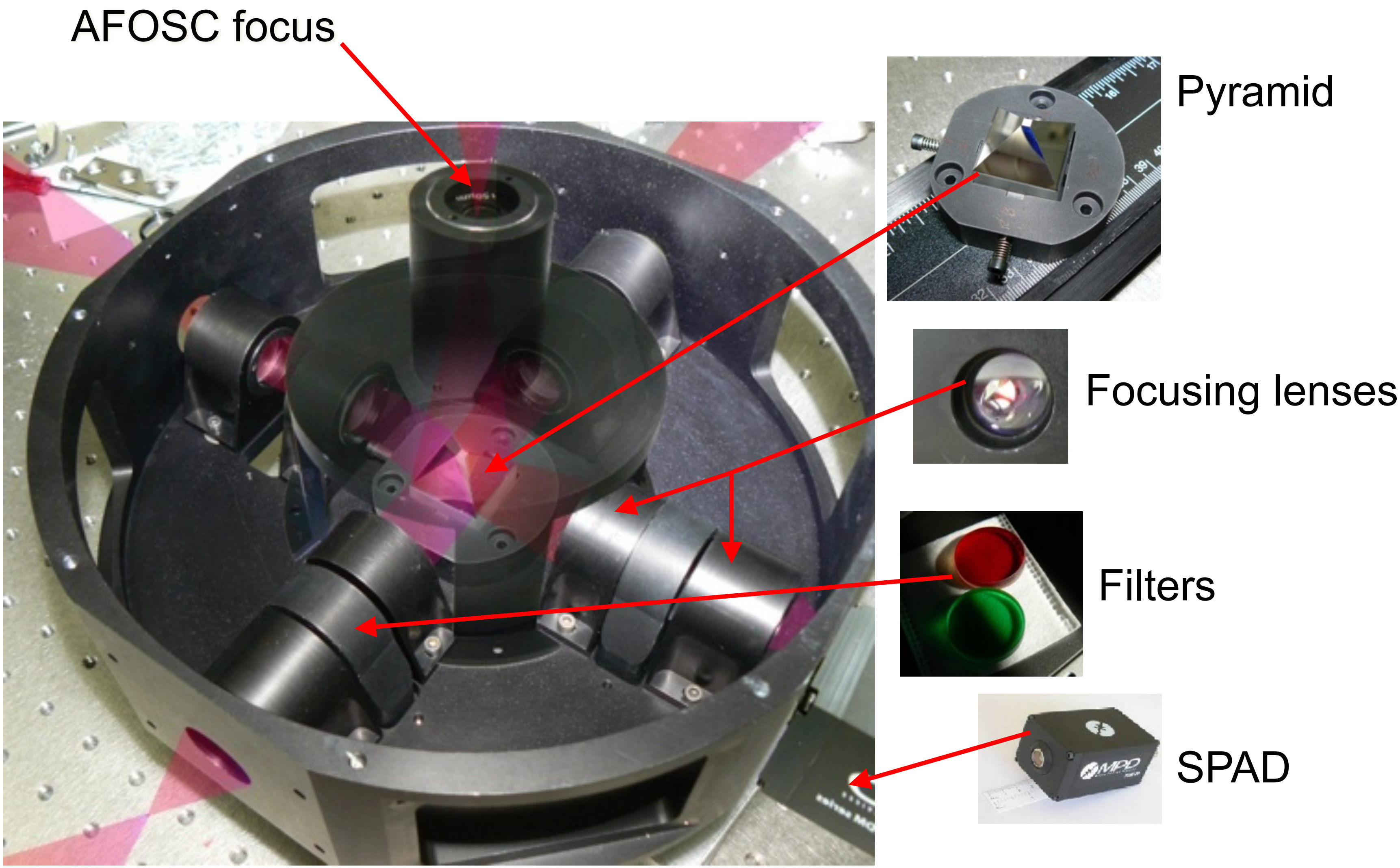

MPD’s SPADs

The Geiger mode MPD SPADs are operated in **continuous mode**. The timing circuit and cooling stage are integrated in a ruggedized box. Two output connectors, TTL and NIM, can be operated in parallel. NIM connectors have a timing accuracy around **35 ps, 5-10 times better than with the TTL**.

Initially we had only 50 micron sizes, then 100 micron, as in the present configuration. The dark counts are less than 100/s even on the larger SPADs.

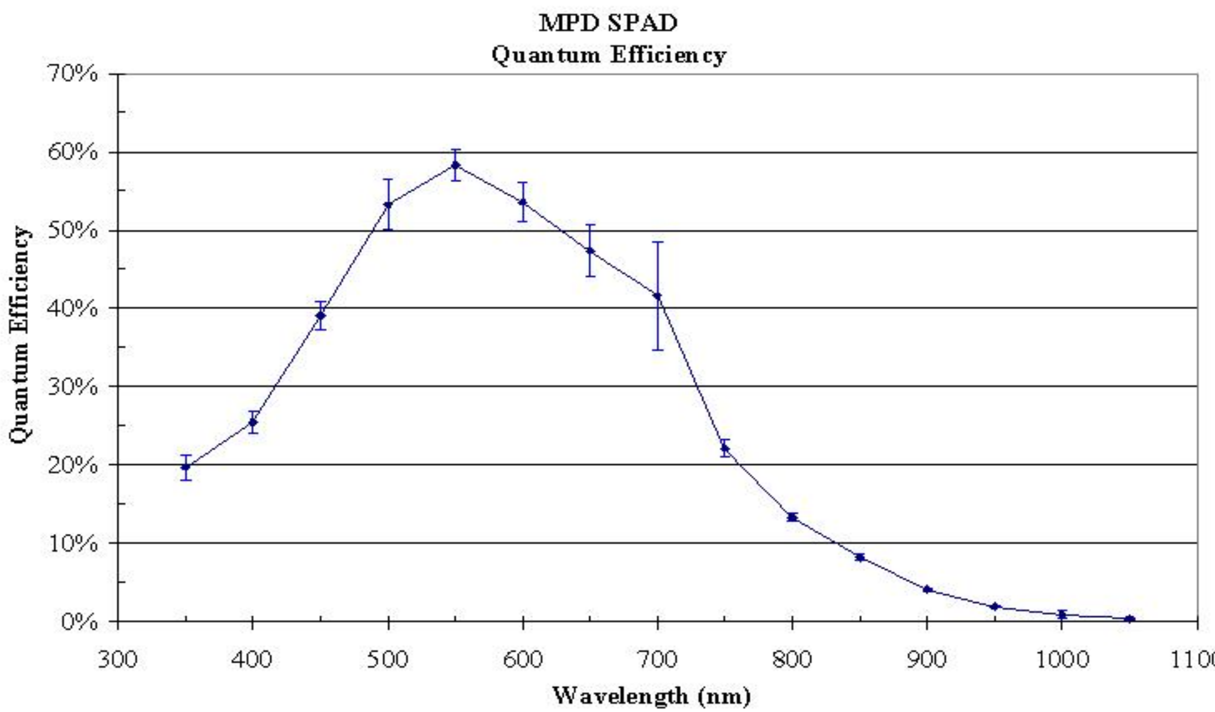

The Quantum Efficiency peaks around 60% in the visible.

Operating modes with four pupils

By taking advantage of the split.pupil concept**, each time tag** out of each detector is **individually acquired and permanently stored**, and the data are **post-processed with selectable time bins** according to the specific problem**.**

Two scientific modes have been implemented:

1 - ***simultaneous multicolor photometry*** and ***cross correlation of the 4 sub-apertures (Intensity Interferometry)***.
2 – when summing together the 4 outputs, usually in white light, an increased ***S/N ratio and dynamic range***, and a ***partial recovery of the dead time***

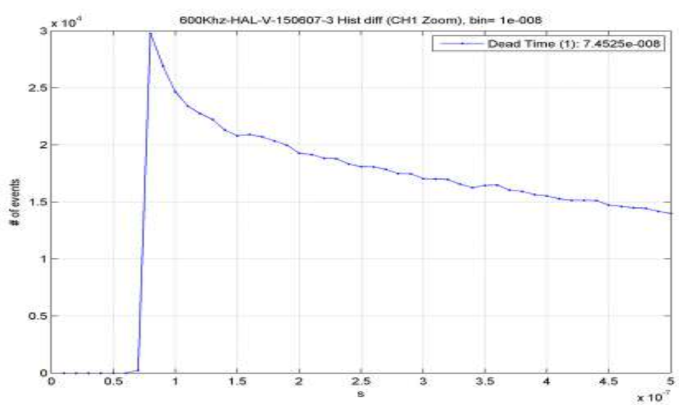

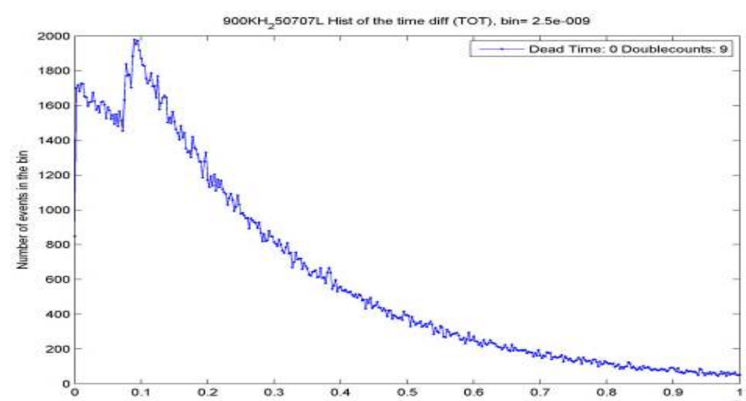

The overall system

A TDC board made by CAEN for CERN

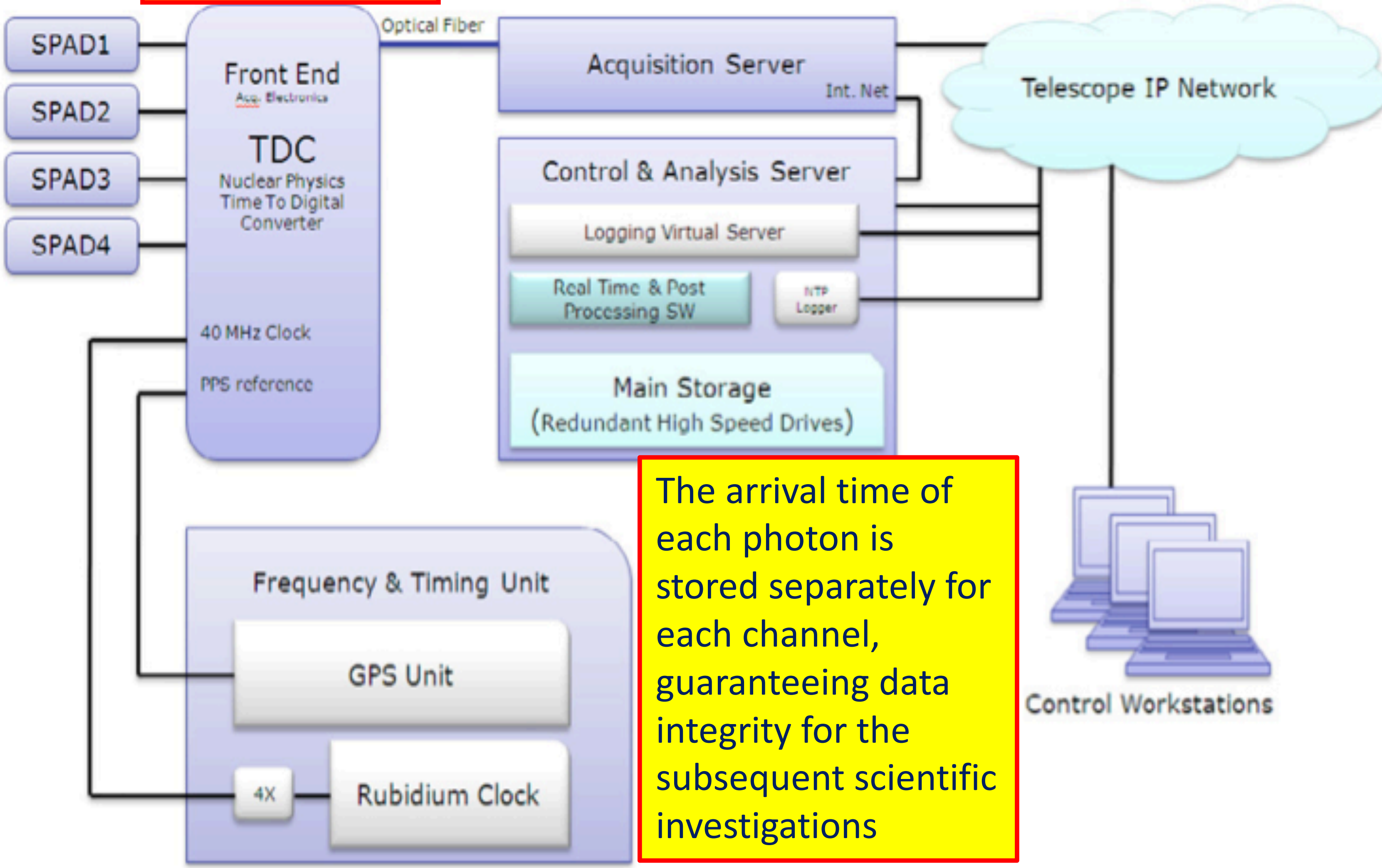

The arrival time of each photon is stored separately for each channel, guaranteeing data integrity for the subsequent scientific investigations

Acquisition and Time System

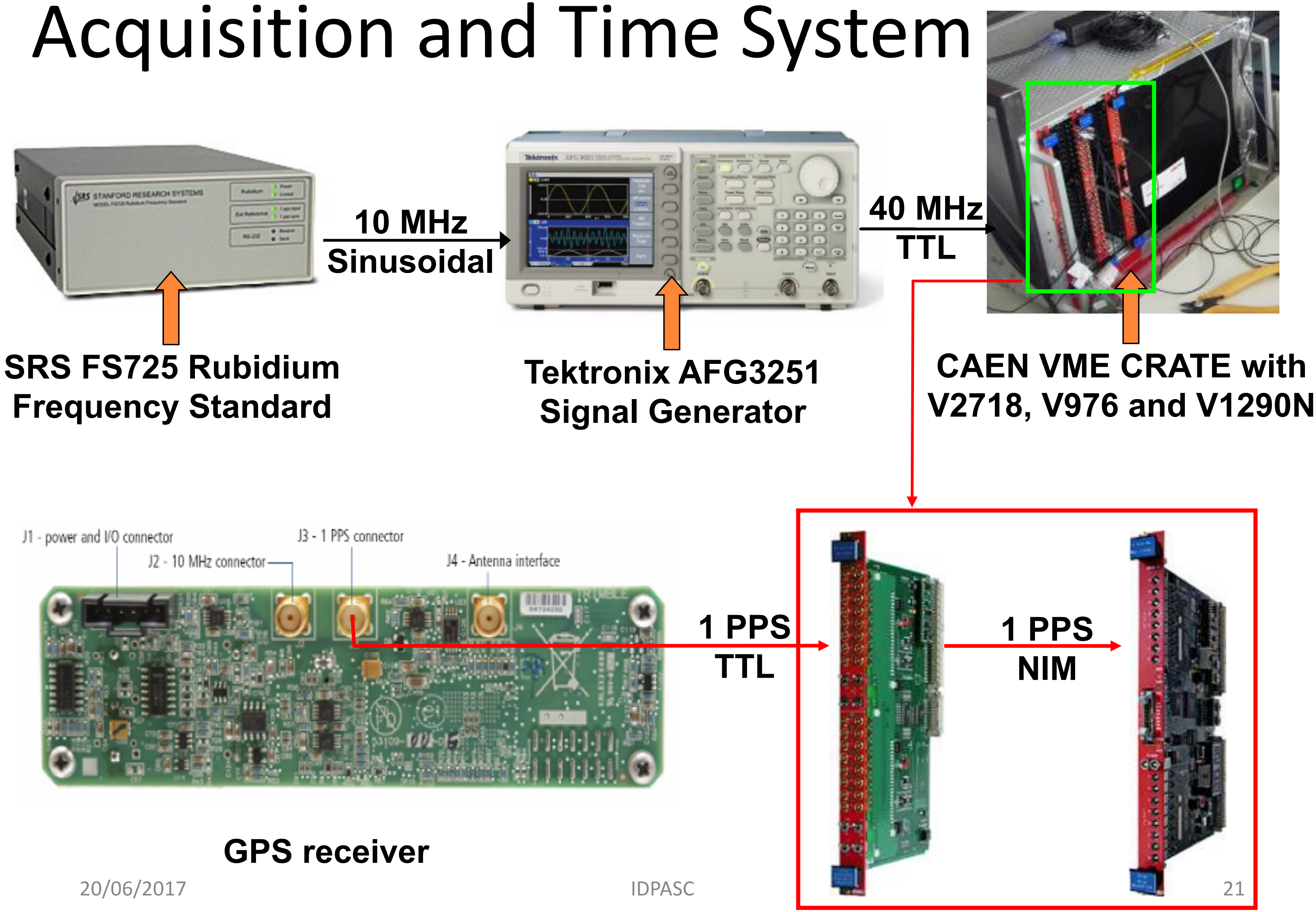

AquEYE

AquEYE, the Asiago Quantum Eye.

It was originally mounted on the focal plane of the imaging spectrograph AFOSC of the Asiago-Cima Ekar (Italy) 182 cm Copernicus telescope in place of the CCD camera.

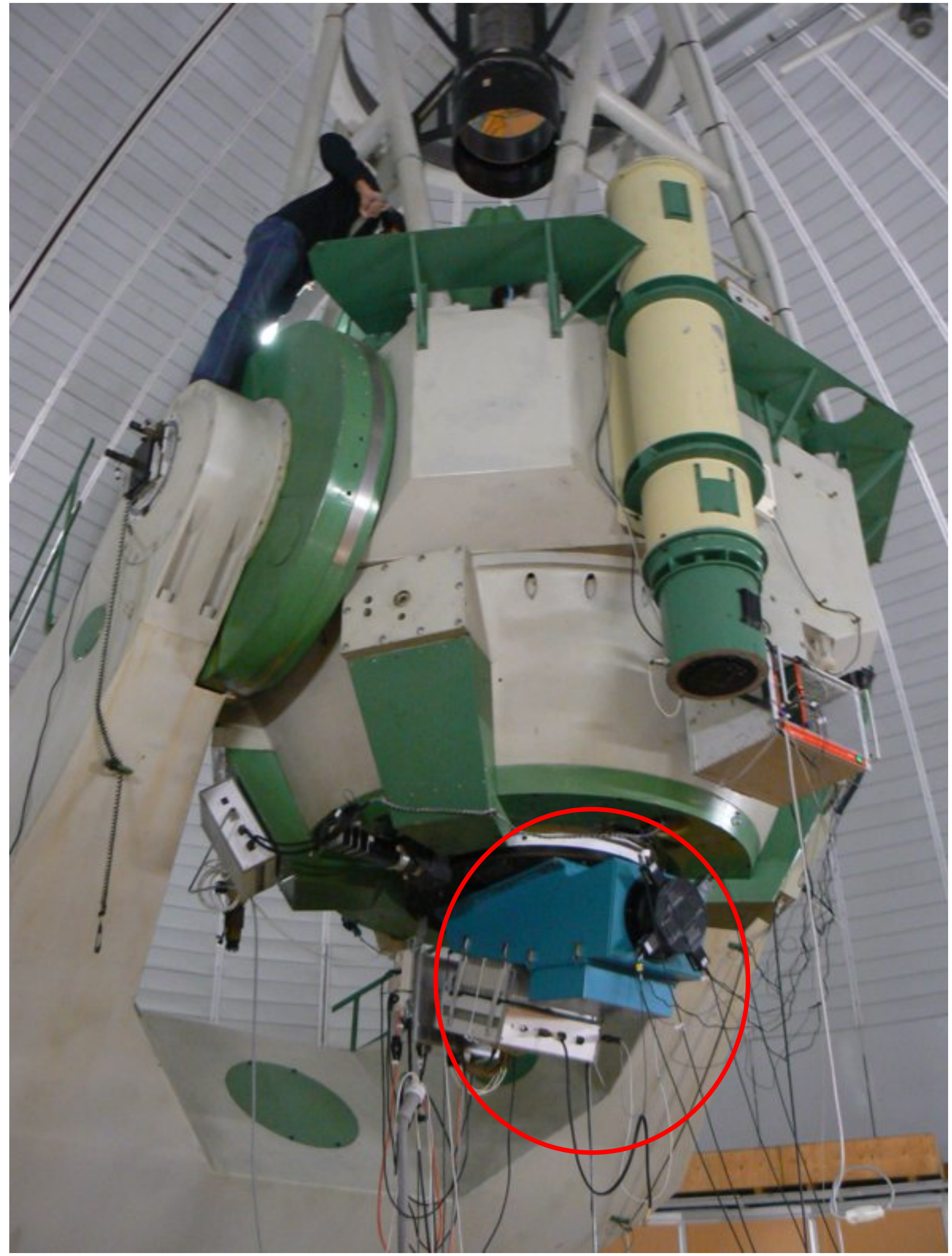

A more detailed view

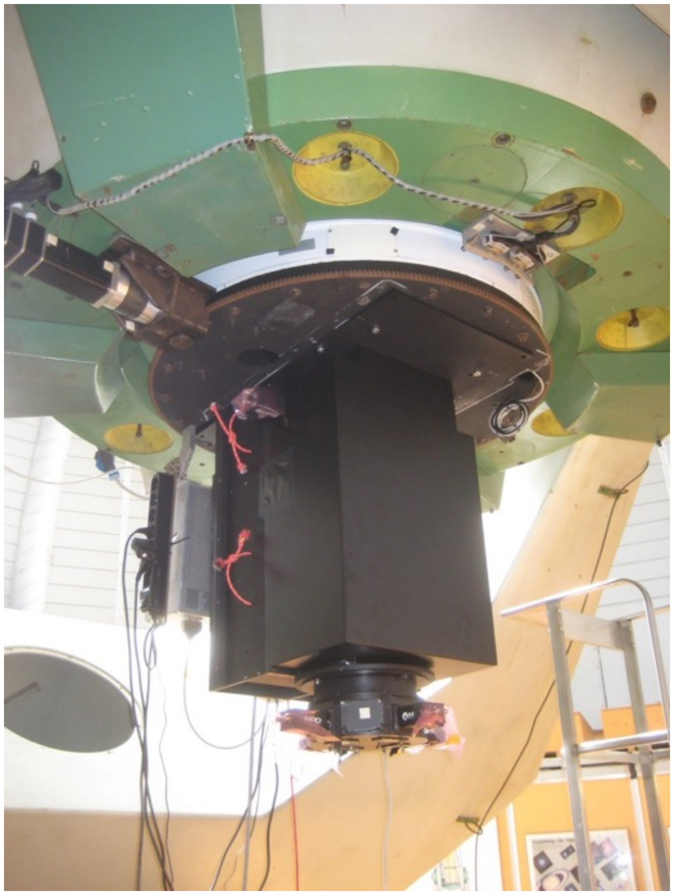

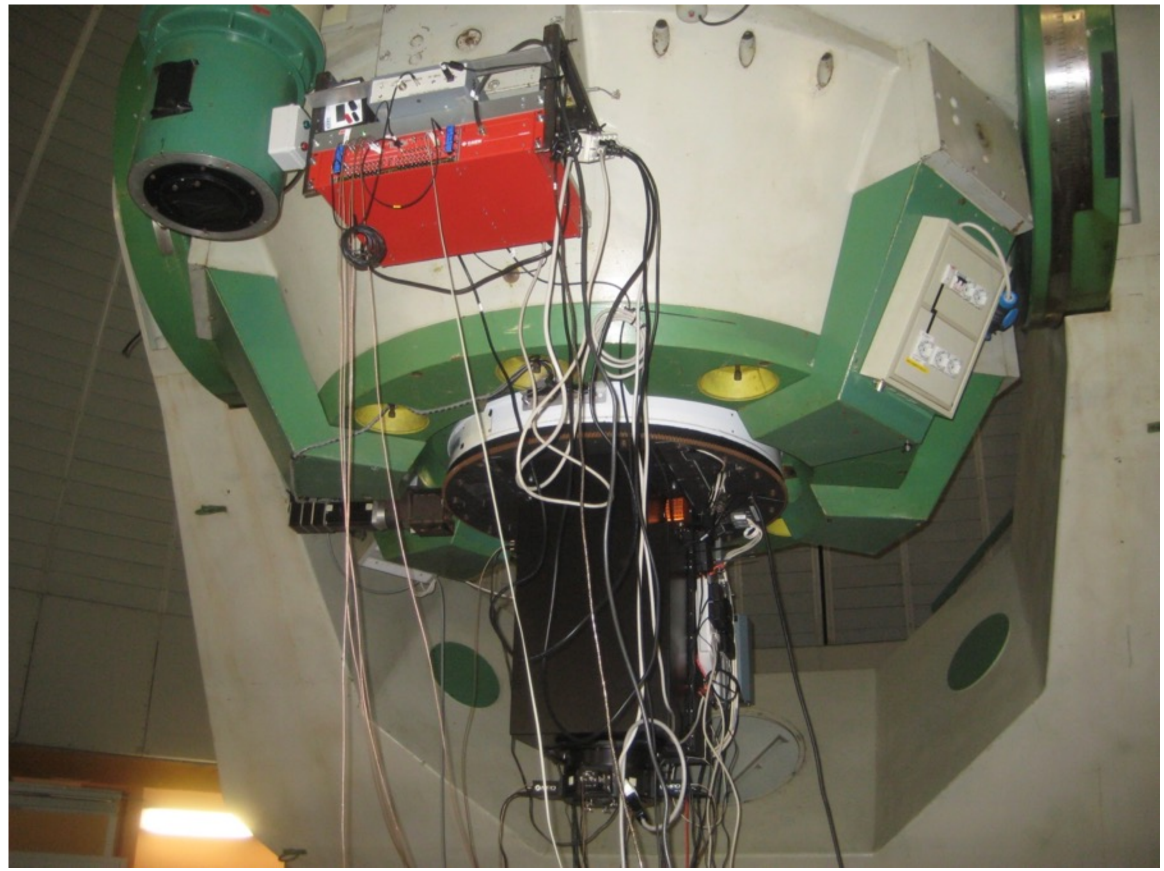

Iqueye for the NTT

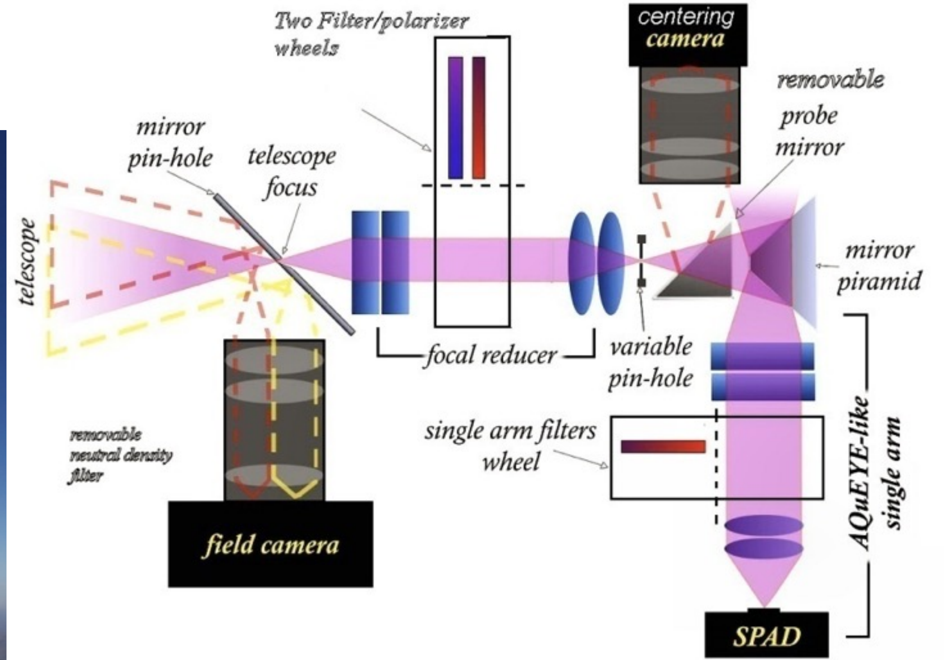

Thanks to the positive experience of AquEYE, it was decided to realize IquEYE, a more complex instrument for applications to a larger telescope, namely the ESO 3.5m NTT in La Silla (Chile). The same basic optical solution of pupil splitting in 4, and overall system architecture, were maintained. Most important additions were a 5th SPAD to monitor the sky and a guiding camera.

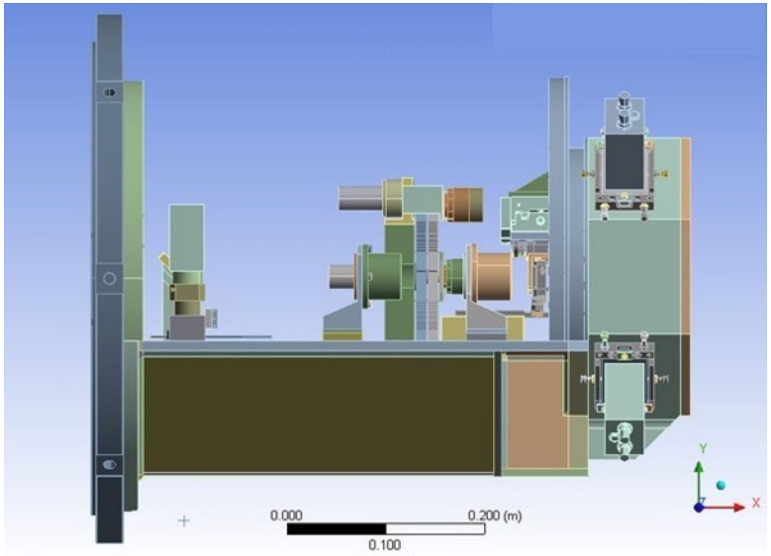

IquEYE optomechanics

As for Aqueye, the system is so reliable that operation can be performed from a control room several km away from the telescope

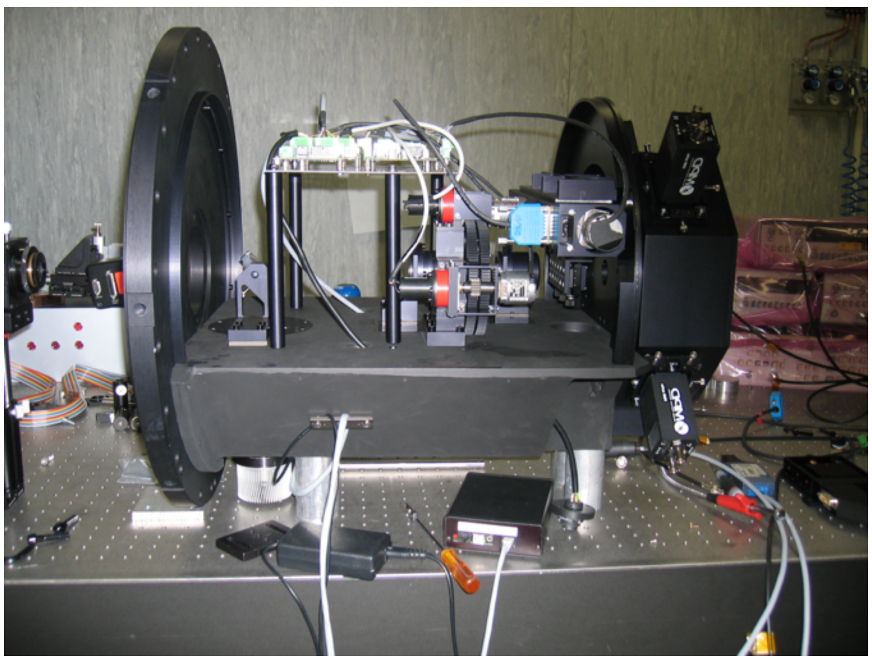

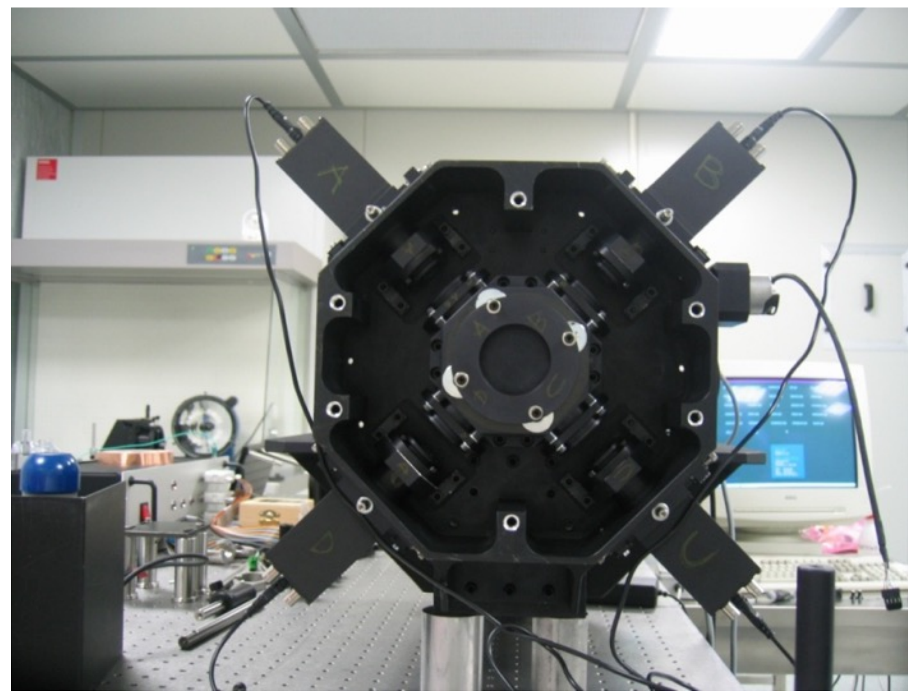

Present status of Aqueye and Iqueye

Aqueye has been upgraded to Aqueye+ with the addition of a fifth spad and acquisition camera.

Iqueye is back in Asiago and mounted at the 1.2 m Galileo Telescope at Pennar.

Both photometers are fibre-fed from the telescope and located in dedicated controlled rooms.

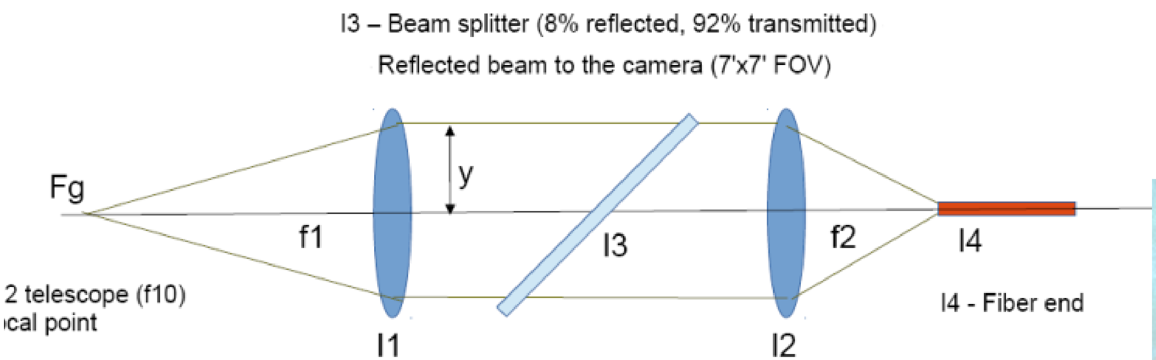

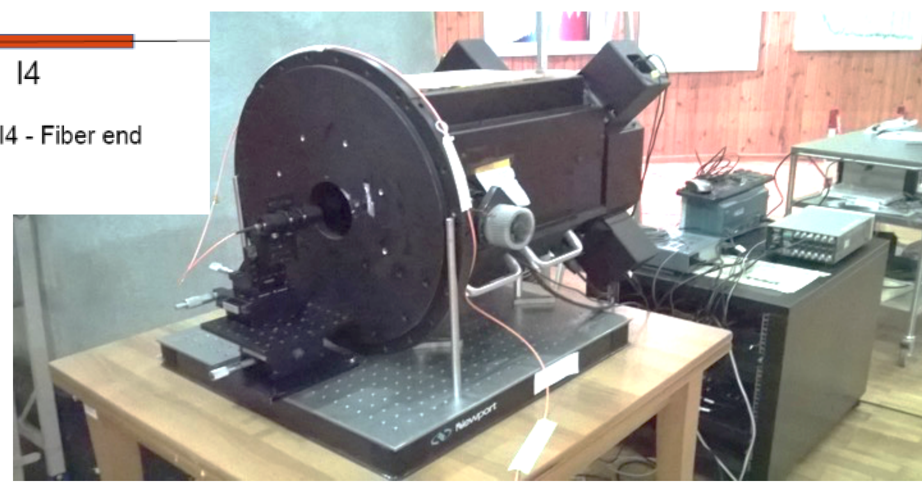

Another fundamental topics for Astronomy: the angular resolution

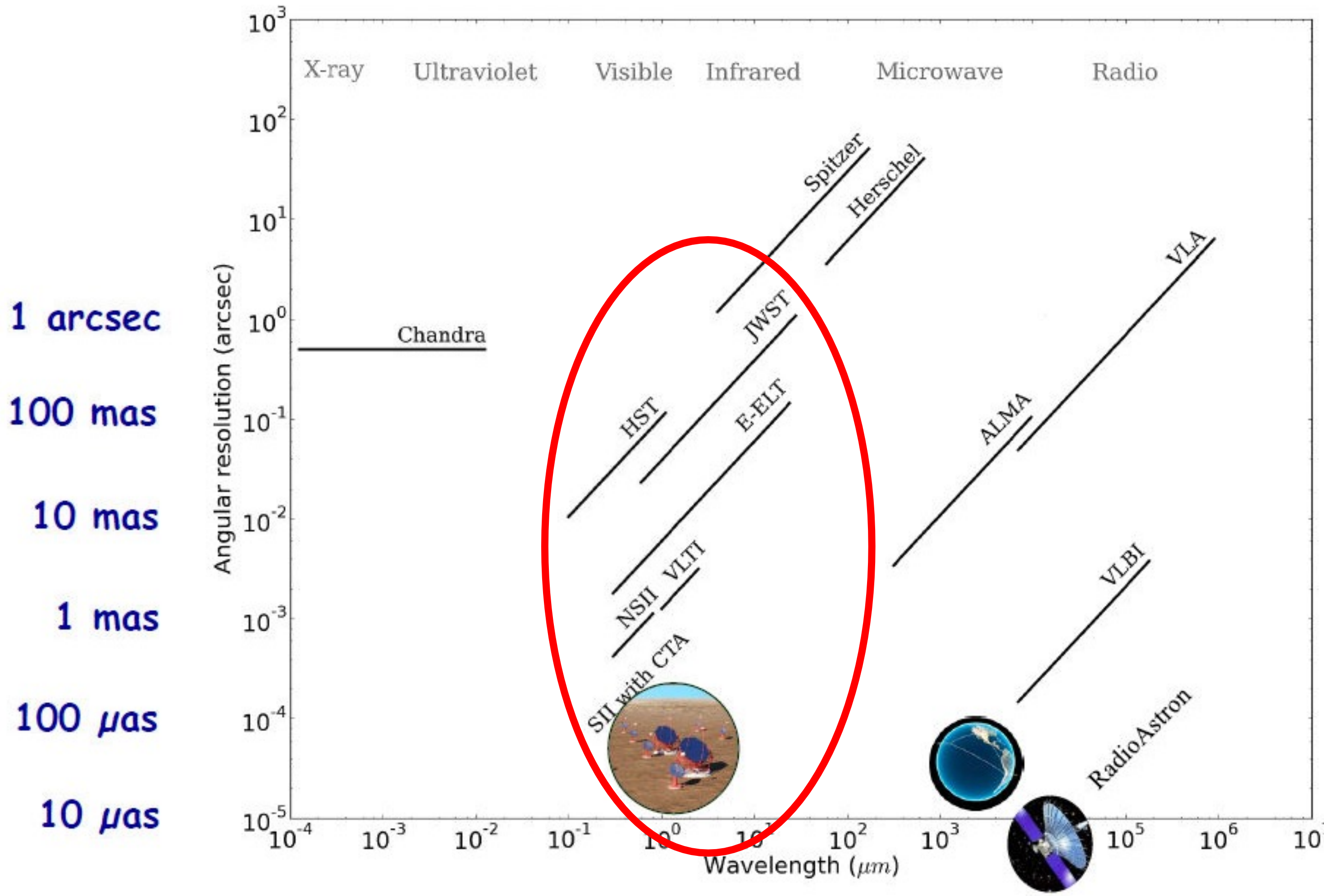

1 radian = 2.06×10^5 arcsec , 1 arcsec = 5 microrad

INTERFEROMETRY

an astronomical application of two-slit interferometry

Michelson (wave)

vs

SII (quantum)

In the radio or far-IR regime, we cannot speak of ‘photons’, so that wave interferometry is more apt in these fields.
‘Photons’ are better employed in the optical, UV, X and Gamma astronomy.

	Single telescope	**Array of N telescopes**
Angular resolution, θ	$\sim \lambda/D$	$\sim\lambda/D_{max}$
Collecting area	$\sim D^2$	$\sim ND^2$

From brightness to visibility - 1

1. An Interferometer measures the interference pattern produced by two apertures.
2. The interference pattern is directly related to the source brightness. In particular, for small fields of view the complex visibility, V(u,v), is the 2D Fourier transform of the brightness on the sky, T(x,y) (van Cittert-Zernike theorem)

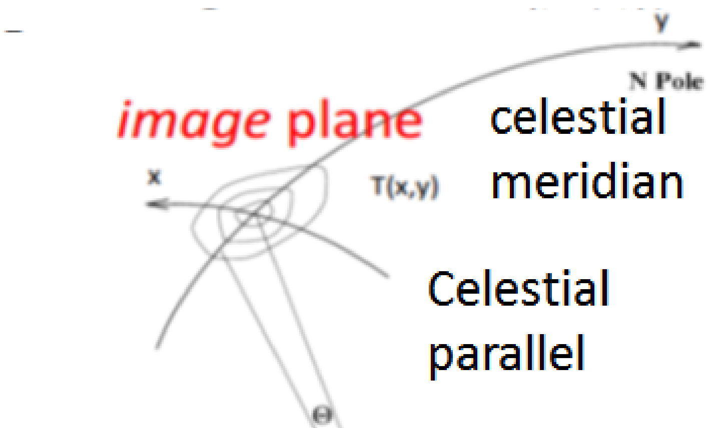

Fourier space/domain

$$V(u,v) = \int\int T(x,y)e^{2\pi i(ux+vy)}dxdy$$

Image space/domain

$$T(x,y) = \int\int V(u,v)e^{-2\pi i(ux+vy)}dudv$$

From brightness to visibility - 2

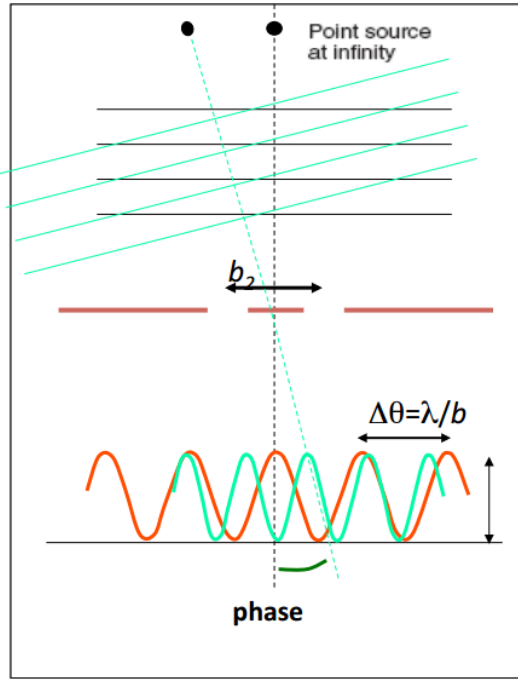

$$|V| = \frac{I_{\max} - I_{\min}}{I_{\max} + I_{\min}} = \frac{\textit{Fringe Amplitude}}{\textit{Average Intensity}}$$

The visibility is a complex quantity:

- amplitude tells "how much" of a certain frequency component
- phase tells "where" this component is located

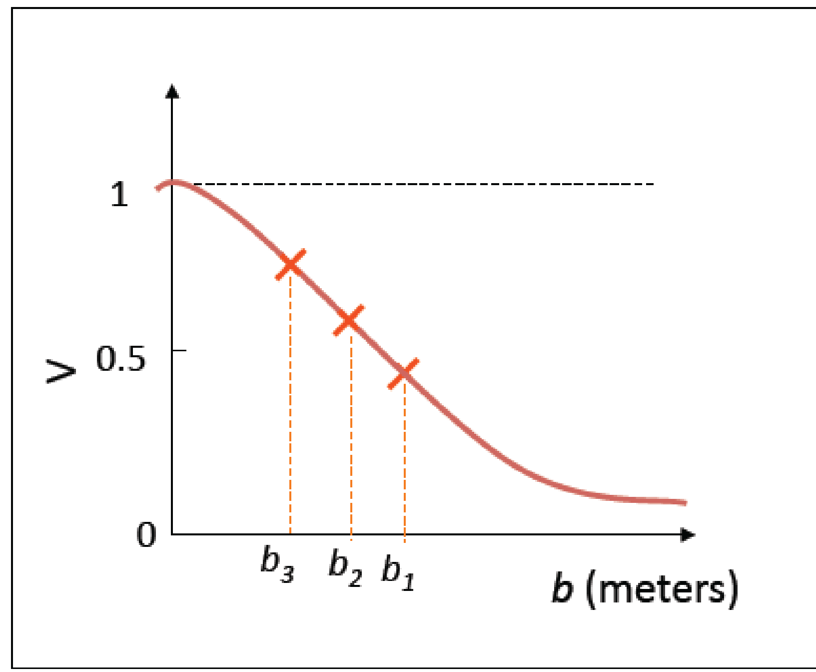

A source is resolved when the visibility goes to zero on the longest baseline.

For example, in the case of a binary system, this corresponds to the angular separation of $\theta = \lambda/2B$.

Aperture synthesis

$$T(x,y) = \int \int V(u,v) e^{-2\pi i(ux+vy)} du dv$$

V(u,v) can be measured on a discrete number of points. A good image quality requires a good coverage of the *uv* plane. We can use the earth rotation to increase the *uv* coverage

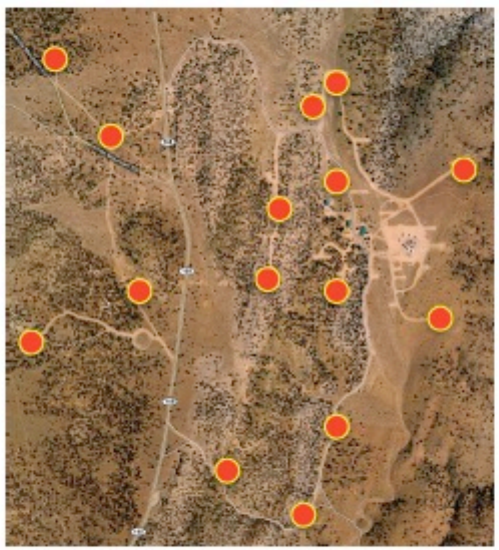

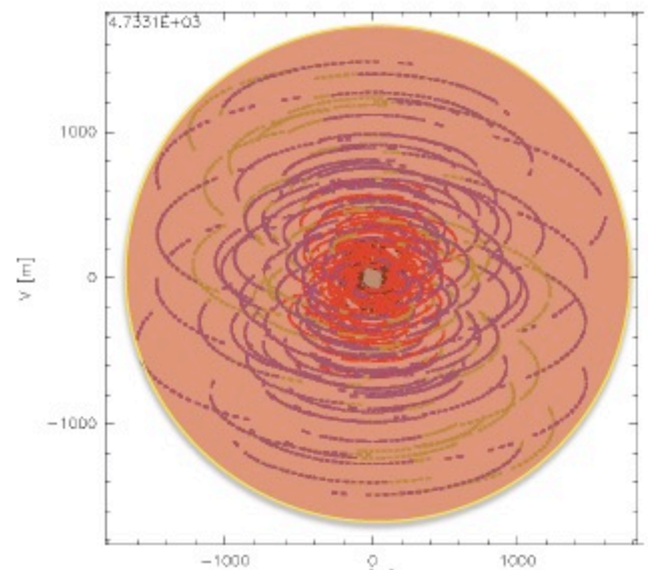

The original Michelson Interferometer on the 2.5m telescope of Mt. Wilson

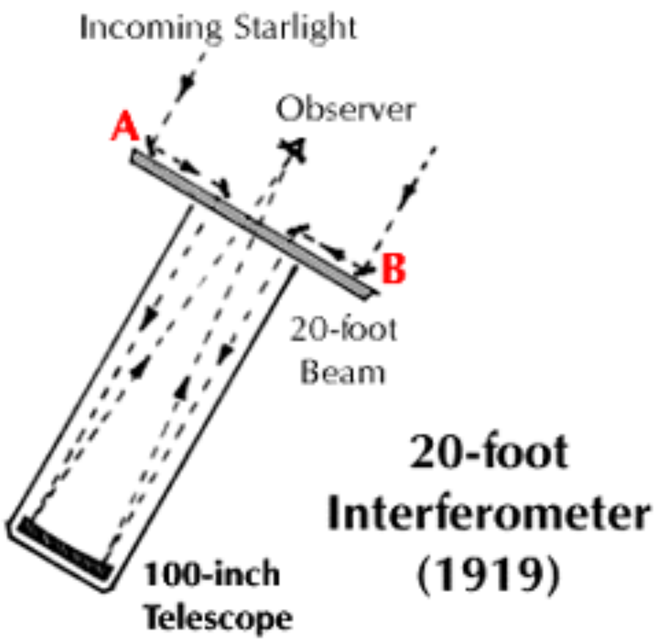

Small mirrors on the 20-foot beam directed light into the telescope. The effective diameter of the telescope has now become the distance between mirror A and B.

The 20-foot beam on top of the 100-inch Hooker Telescope on Mt. Wilson in Southern California.

Almost 100 years ago, Michelson could measure for the first time few stellar diameters of giant (red) stars

Modern Michelson interferometers

Main improvements are the capability to compensate the light path difference along the beams, and the detectors

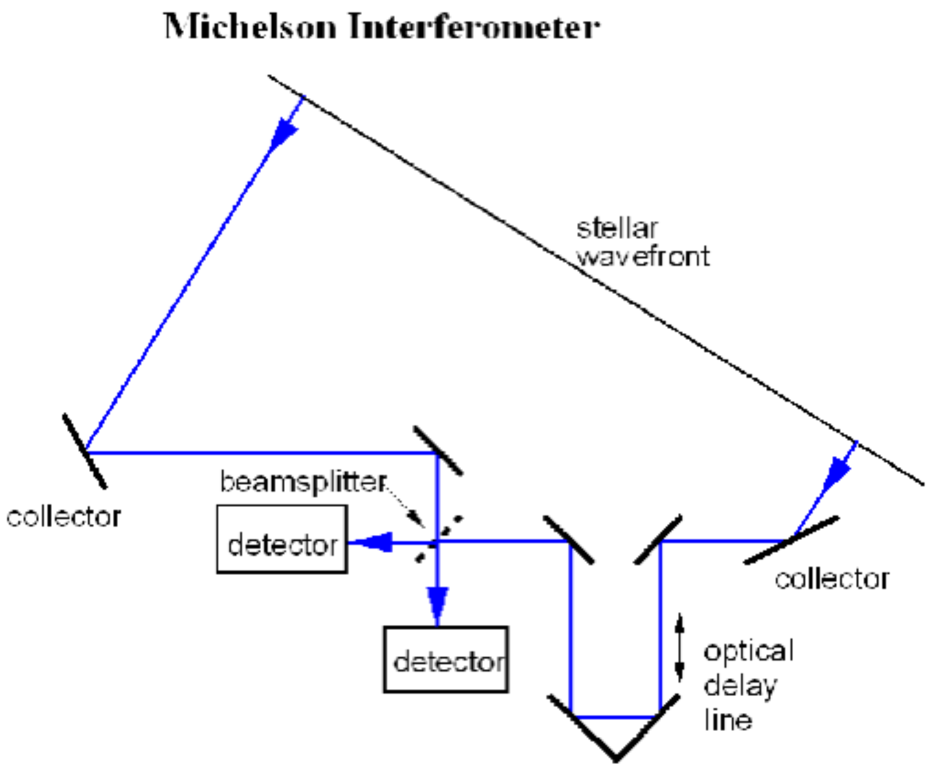

The light paths must be very accurately controlled to a **fraction of wavelength** (e.g. sending light from the telescope through carefully thermostated vacuum pipes). **The longer is λ, the easier is to achieve good coherence.** Therefore Michelson type interferometers are particularly suited in the near infrared (e.g. K band) for ***red stars***.

The CHARA Interferometer at Mt. Wilson

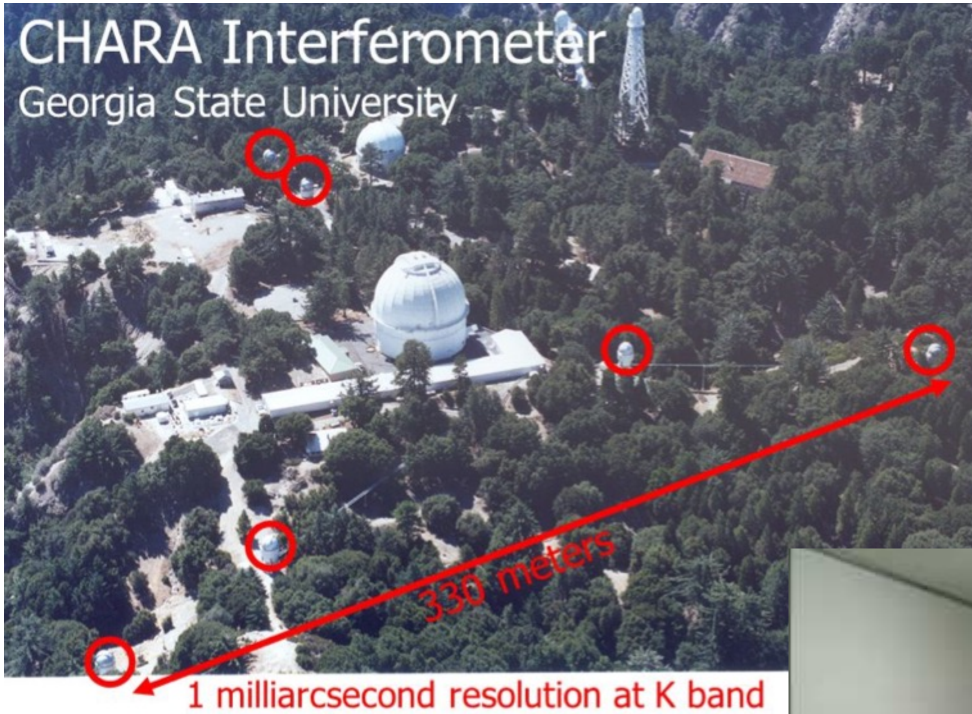

The Keck Interferometer at Mauna Kea

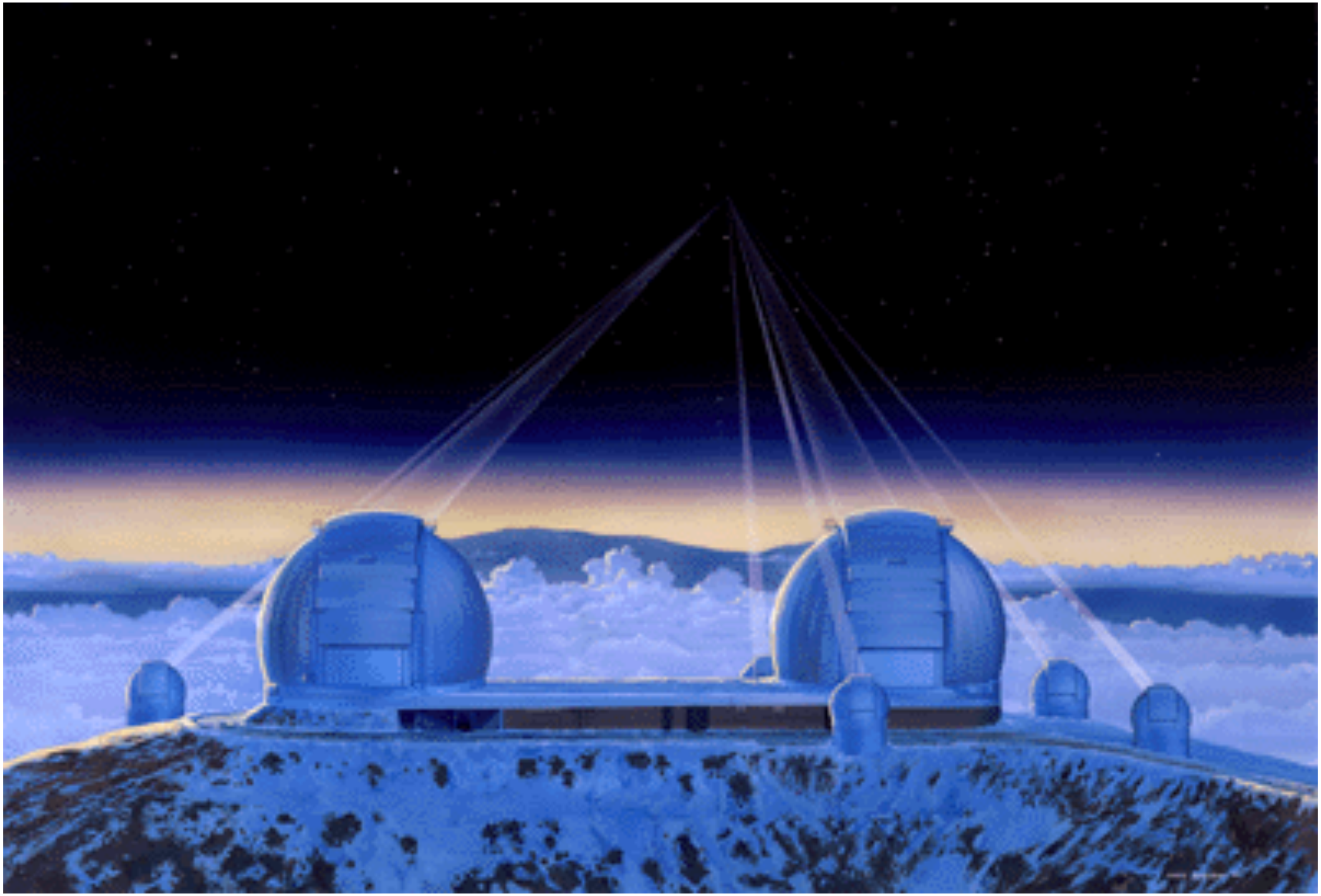

The interferometric configuration of the VLT

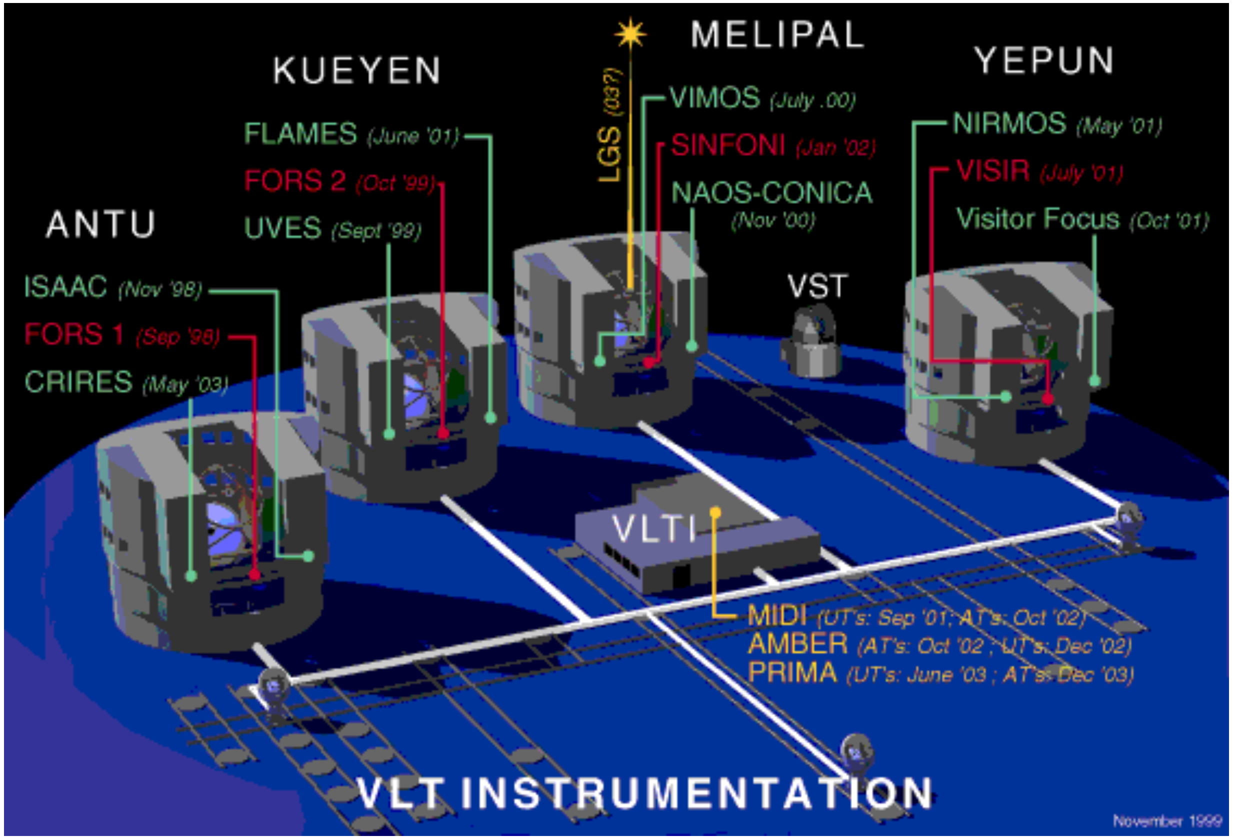

The 4 telescopes can operate separately or in interferometric configuration. The disposition of the 4 telescopes on ground was meant for an optimal coverage of the (u,v) plane given 4 apertures.

Three smaller 1.8m auxiliary telescopes, movable on rails, help to fill the (u,v) plane .

The VLTI underground laboratory

The U.S. Navy Precision Optical Interferometer

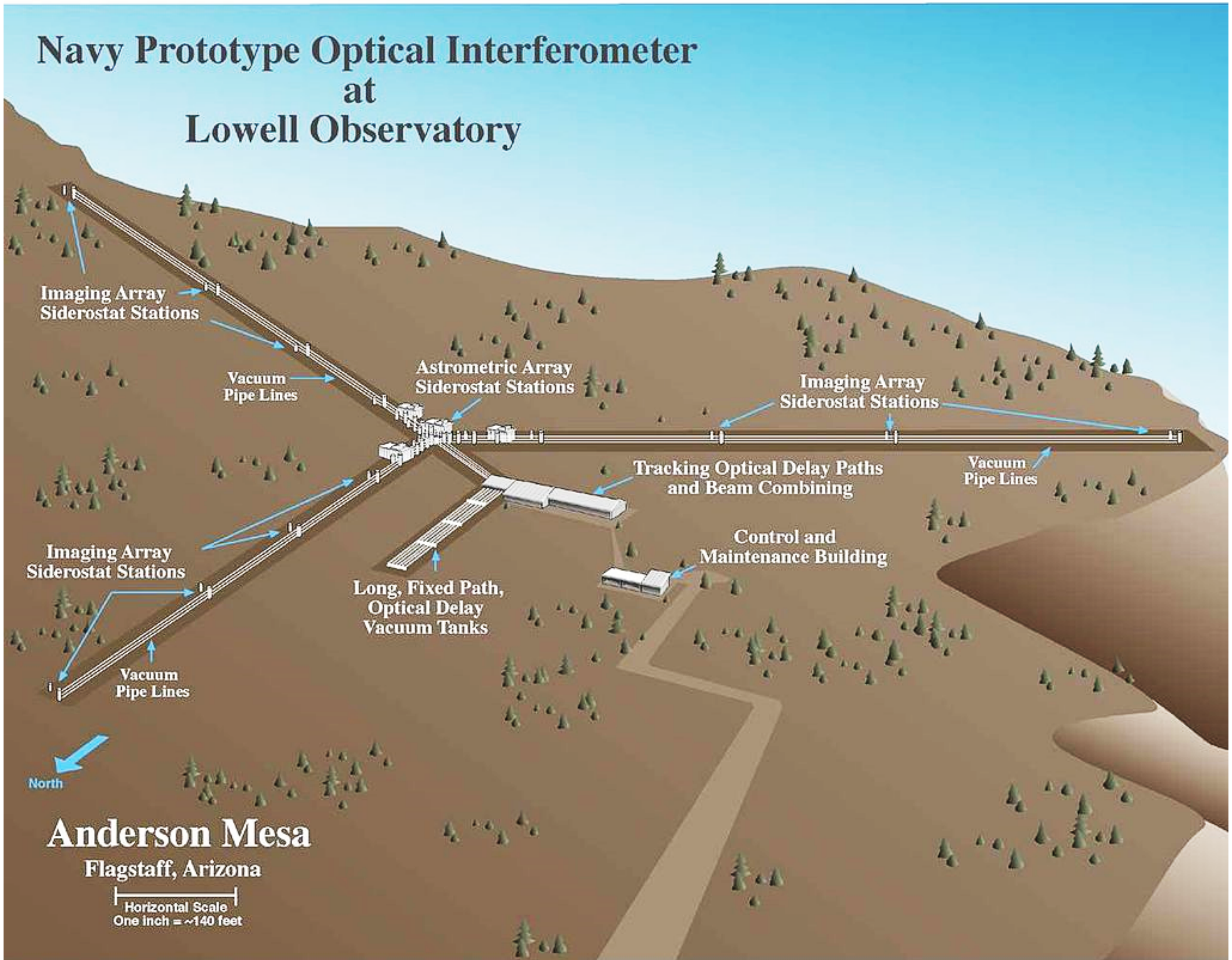

Fringes from stars and extended disks

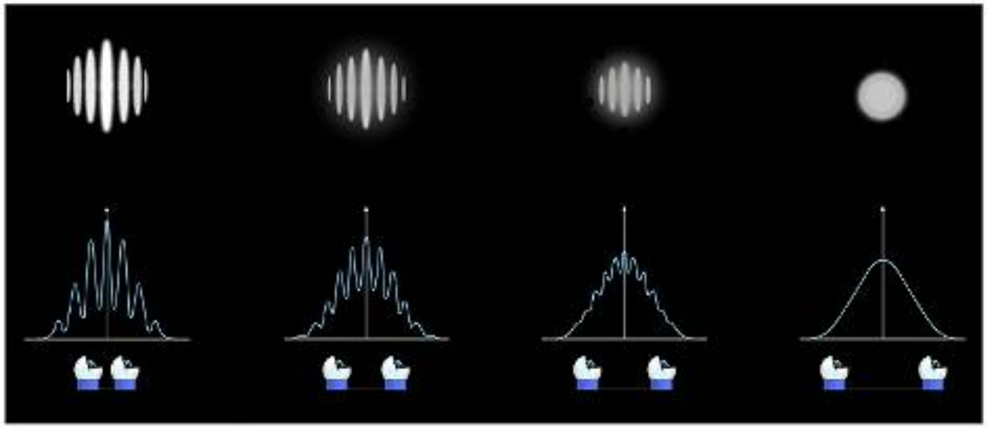

Interferometric Fringes at Different Telescope Baselines
(Simulation)

ESO PR Photo 10e/01 (18 March 2001)

© European Southern Observatory

Here some simulations of point-like stars and extended disks at different baselines.

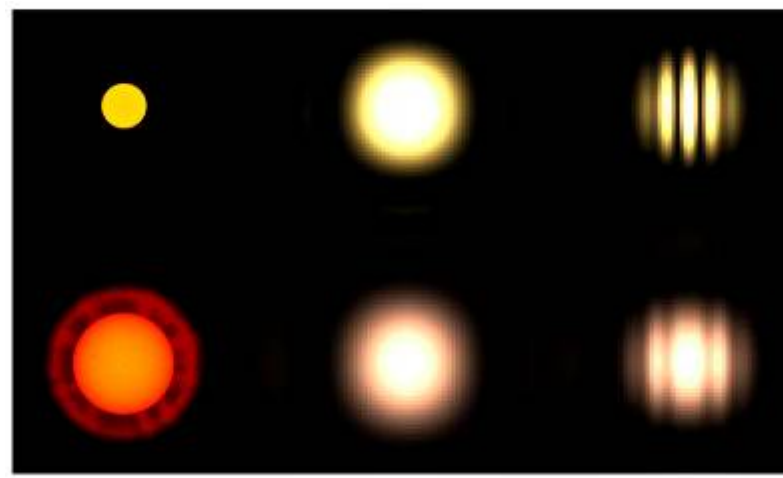

Interferometric Fringes from Star with Different Angular Diameters
(Simulation)

ESO PR Photo 10d/01 (18 March 2001)

© European Southern Observatory

Two examples of bright resolved stars by Michelson interferometers

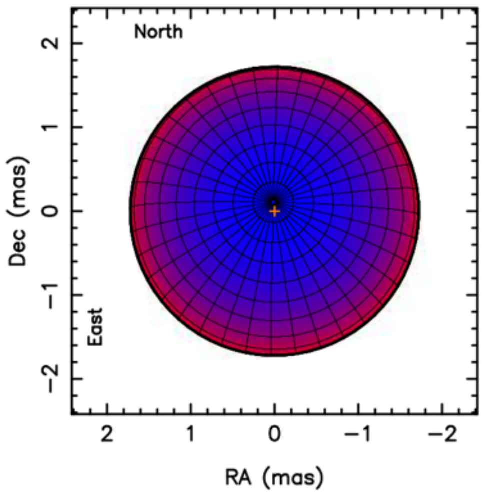

A false color model of Vega from NPOI observations. The temperature drops more than 2400 K from pole to equator. Polar diameter is only 80% of the equator (Peterson et al. 2006).

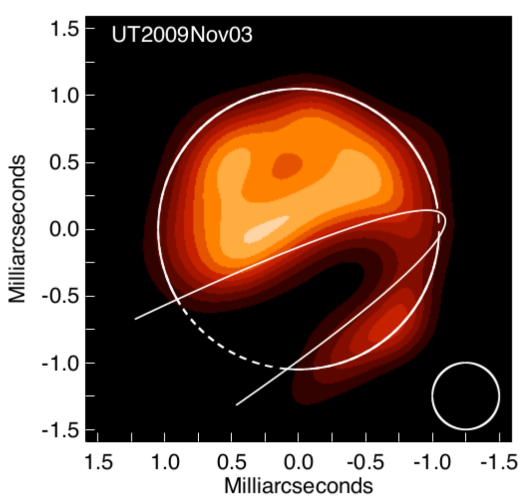

CHARA (Mt. Wilson) interferometric image of a 18-month long partial eclipse of ε Aur from a disc orbiting the companion (Kloppenborg et al. 2010).

Intensity Interferometry

VOLUME 10, NUMBER 3 PHYSICAL REVIEW LETTERS 1 FEBRUARY 1963

PHOTON CORRELATIONS*

Roy J. Glauber
Lyman Laboratory, Harvard University, Cambridge, Massachusetts
(Received 27 December 1962)

In 1956 Hanbury Brown and Twiss[1] reported that the photons of a light beam of narrow spectral width have a tendency to arrive in correlated pairs. We have developed general quantum mechanical methods for the investigation of such correlation effects and shall present here results for the distribution of the number of photons counted in an incoherent beam. The fact that photon correlations are enhanced by narrowing the spectral bandwidth has led to a prediction[2] of large-scale correlations to be observed in the beam of an optical maser. We shall indicate that this prediction is misleading and follows from an inappropriate model of the maser beam. In considering these problems we shall outline a method of describing the photon field which appears particularly well suited to the discussion of experiments performed with light beams, whether coherent or incoherent.

The correlations observed in the photoionization processes induced by a light beam were given a simple semiclassical explanation by Purcell,[3] who made use of the methods of microwave noise theory. More recently, a number of papers have been written examining the correlations in considerably greater detail. These papers[2,4-6] retain the assumption that the electric field in a light beam can be described as a classical Gaussian stochastic process. In actuality, the behavior of the photon field is considerably more

The first paper by Glauber made reference to the 1956 HBT experiment, whose application to the astronomical field became ***Intensity Interferometry*** (HBTII) in Narrabri (Australia) .

Correlation in Intensity Interferometry

It can be shown that the second order correlation (Intensity Interferometry) is proportional to $|\gamma|^2$, namely to the square of the ***fringe visibility in the Michelson interferometer***:

$$\gamma^{(2)}(\mathbf{r}_1,\mathbf{r}_2,\tau)=\frac{\langle I(\mathbf{r}_1,t)I(\mathbf{r}_2,t+\tau)\rangle}{\langle I(\mathbf{r}_1,t)\rangle\langle I(\mathbf{r}_2,t+\tau)\rangle}=1+|\gamma|^2\leq 2$$

$|\gamma|^2$ can be measured using ***photon counts***, by introducing the **discrete degree of coherence**:

$$\mathbf{g^{(2)} = n\cdot N_{AB} /(N_A N_B)}$$

where N_A, N_B = number of photons detected at telescopes A and B in time T,
N_{AB} = number of "simultaneous" detections in small time bins dt in T,
n = number of intervals (T/dt)

Observational consequences

Expressing N_A, N_B and N_{AB} in terms of the average intensities

$<I_A>$, $<I_B>$, $<I_A I_B>$,

and integrating over time T:

$$N_{AB} = (1/T)\, N_A N_B \,(dt + 0.5 \int |\gamma|^2 \, d\tau)$$

$$\mathbf{g^{(2)}} = 1 + 0.5/dt \int |\gamma|^2 \, d\tau = 1 + 0.5\gamma^2 \,(\tau_c/dt)$$

where $\tau_c = 1/\Delta\nu = (\lambda/c)(\lambda/\Delta\lambda)$ is the **coherence time**, i.e. the interval over which a signal in a wavelength interval $\Delta\lambda$ may be considered coherent in time.

For optical light ina wavelength range $\Delta\lambda = 1$ nm, the coherence time is $\tau_c \sim 1$ ps.

g(2) function and S/N ratio

The major contribution to N_{AB} comes from random uncorrelated coincidences. The 'signal' is a tiny excess of coincidences related to the quantum nature of light (bosons giving a joint detection probability greater than that for two independent events):

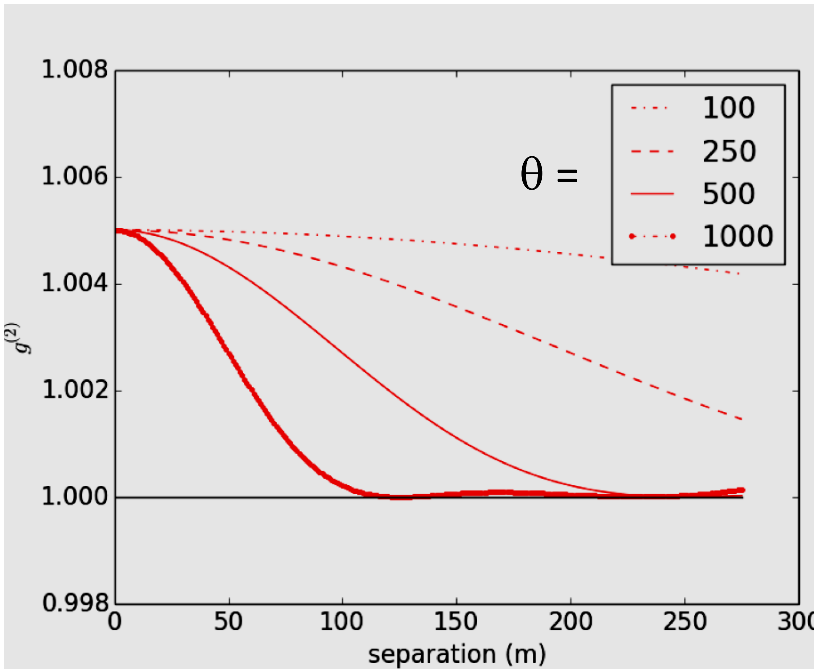

Degree of coherence (**ordinate**) as a function of the telescope separation **d** **(abscissa)** for different angular sizes of the source θ (inset, in μarcsec)

$$S/N = n\, A\, \alpha\, |\gamma|^2\, [T/(2\, dt)]^{1/2}$$

Signal-to-noise ratio:

n: flux of photons (counts/m^2/s/Hz)

A: telescope area

α: detector efficiency

Sensitivity grows with ***area*** of telescope and square root of ***electrical bandwidth***

The Narrabri Intensity Interferometer

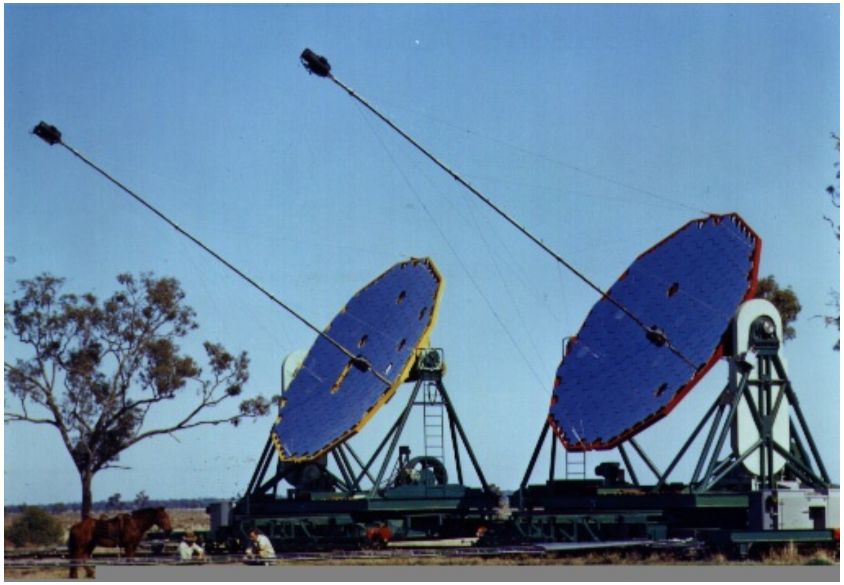

A 'stellar interferometer' was completed in 1965 at Narrabri, Australia, by R. Hanbury Brown and R. Q. Twiss. By the end of the decade it had measured the angular diameters of more than 30 stars, including Main Sequence **blue stars**. The light-gathering power of the 6.5 m diameter mirrors, the detectors (photomultipliers, the most-used optical filter was (443±5) nm), analog electronics etc. allowed to reach magnitude +2.0, a fairly bright limit indeed.

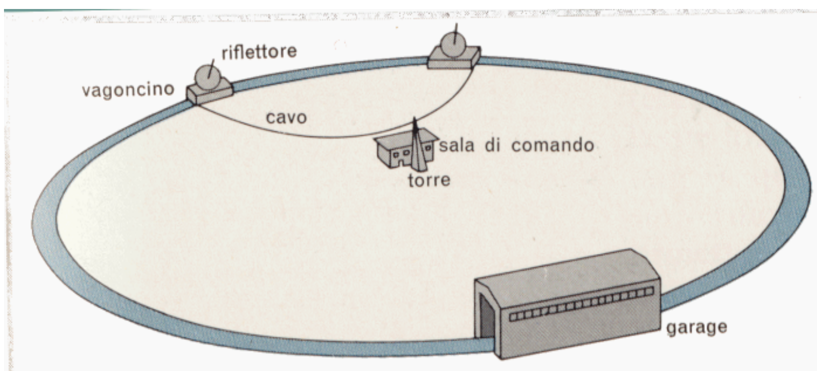

The separation of the mirrors could be varied from 10 m up to 188 m. A central cabin was connected to the carriages by **TV-type coaxial cables**. The available baseline distances permitted measurements of angular diameters from 0.011" to 0.0006".

The currents from the two photomultipliers were multiplied in an analog correlator with a frequency filter that passed a band between 10 and 110 MHz. ***This bandwidth excluded the much lower atmospheric seeing frequencies, thus eliminating their effects.***

Signal-to-Noise ratio and stellar temperature

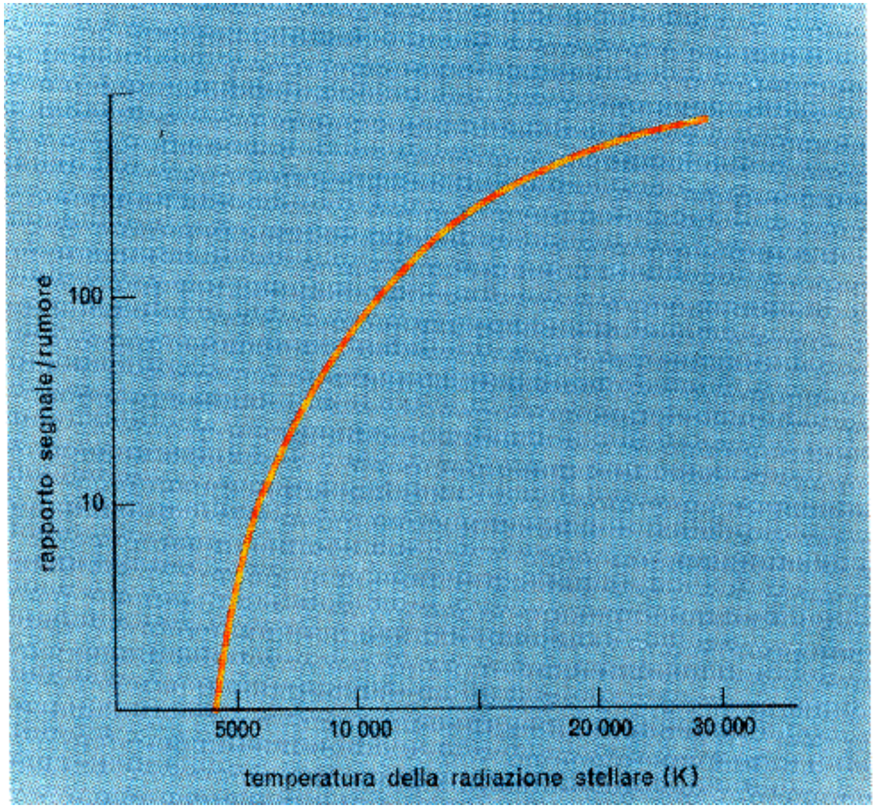

The **S/N R** of intensity interferometry increases with the ***area*** of the telescopes, and the sensitivity increases very rapidly ***with the temperature of the star*** (Bose Einstein statistics), so that ***hot stars gave the best results***.

R.Hanbury Brown, J.Davis, L.R.Allen, J.M.Rome, MNRAS 137, 393 (1967)

Results of HBTII

The *diameter* of the several blue stars were obtained.
If sufficient S/N would have been available, also the *limb darkening* from the second lobe could have been measured.
No sensitivity to Cherenkov light from cosmic rays was noticed.

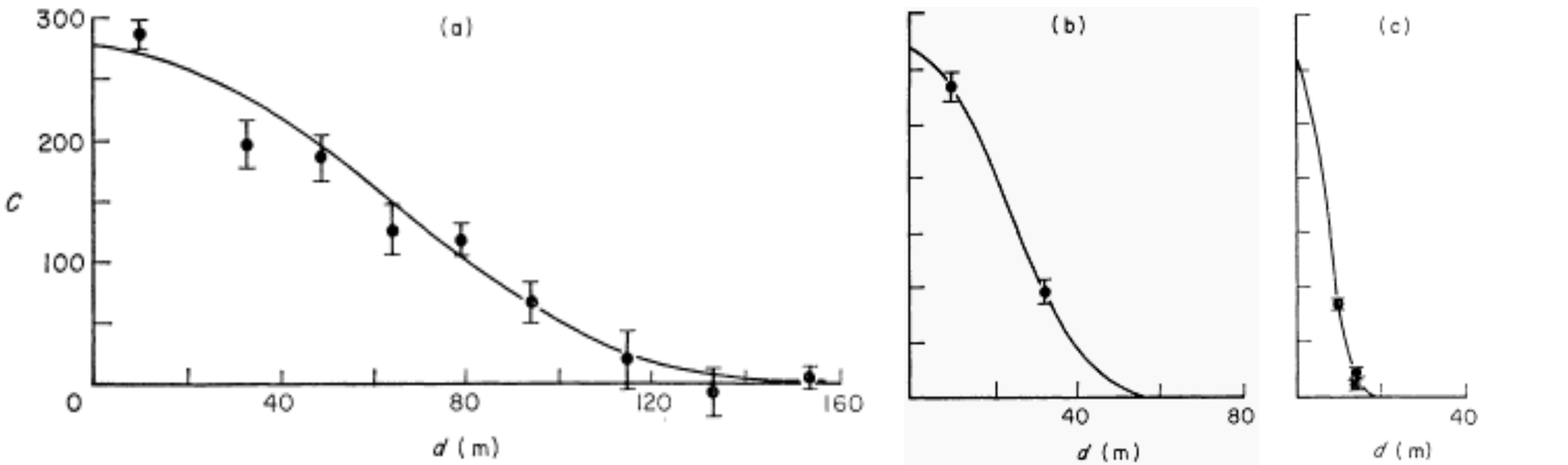

CHANGE OF CORRELATION WITH BASELINE (A) BETA CRU (B0 IV); (B) ALPHA ERI (B5 IV); (C) ALPHA CAR (F0 II).

Expected improvements with a modern HBTII

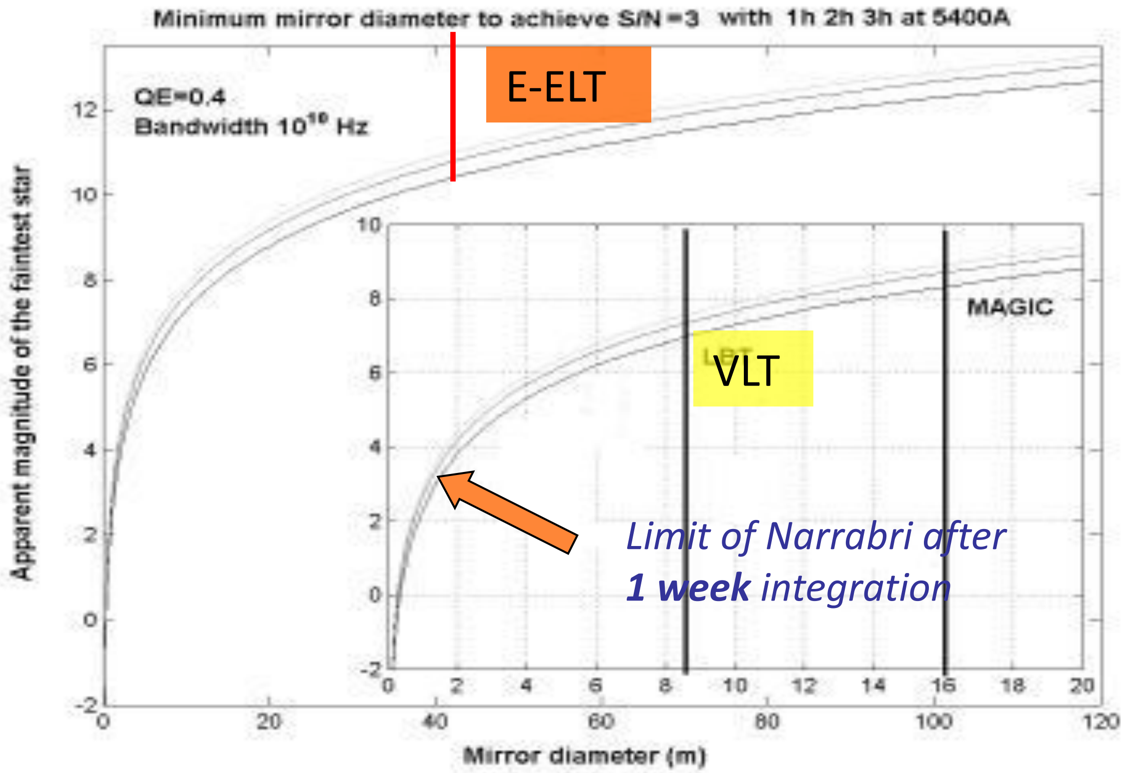

Orders of magnitude improvements in sensitivity with respect to the original Narrabri realization are expected thanks to:

- Higher QE detectors
- Digital electronics with ***higher electrical bandwidth (1-10 GHz)***
- Better optical quality minimizing the background

Scientific goal and potential targets for modern SII

Bright and hot (blue) stars are preferred targets because they not only provide a significant photon flux, but also are compact enough to have a large coherence area and produce significant visibility over 100-1000 m baselines. ***Several thousands of them, brighter than the 7th magnitude, are available.***

For the brightest of them, measurements with an accuracy of ~ 1% are achievable. At this level of accuracy:

- the difference between uniform and limb/gravity-darkened discs is measurable
- stellar model atmospheres can be tested and stellar photospheres can be distinguished from chromospheres, or circumstellar emission regions in discs/winds

At m $\approx$ 10 the brightest nuclei of blue galaxies (Seyfert's) become observable

Main advantages of SII over Michelson’s

- Accuracy is only required for ***electronic bandwidth, not for geometry, precisions of*** a few centimeters, ***not fractions of a wavelength***, are needed
- ***Optical quality*** of the telescope is ***not*** crucial, the limitation is the amount of background light inside the pixel
- ***SII is insensitive to seeing conditions***, on nanosecond timescales the atmosphere is at rest, so that adaptive optics is ***not*** required
- ***No optical link*** between telescopes is necessary, an ***accurate time reference*** is sufficient, either with real-time hardware correlators or software correlators in post processing

Main disadvantages

- **Intrinsic low sensitivity**: a good S/N ratio requires large telescope areas, very efficient detectors, narrow optical bandwidth, very fast electronics

Therefore, Intensity Interferometry is complementary to Michelson’s, and suitable for observations of hot and small sources, specially at short wavelengths.

The Asiago Experiment

A SII photon counting experiment on a 4 km baseline with two Asiago telescopes (Zampieri et al. 2016, Naletto et al. 2016)

. Distance between telescopes ~ 3885 m, with a significant E-W component. The Interferometer has a variable baseline because its projected component perpendicular to the wavefront changes in time, e.g. ~ 2000 m for a source at small elevation at E or W

. Telescopes equipped with our two very fast photon counters: **Aqueye+ and Iqueye**

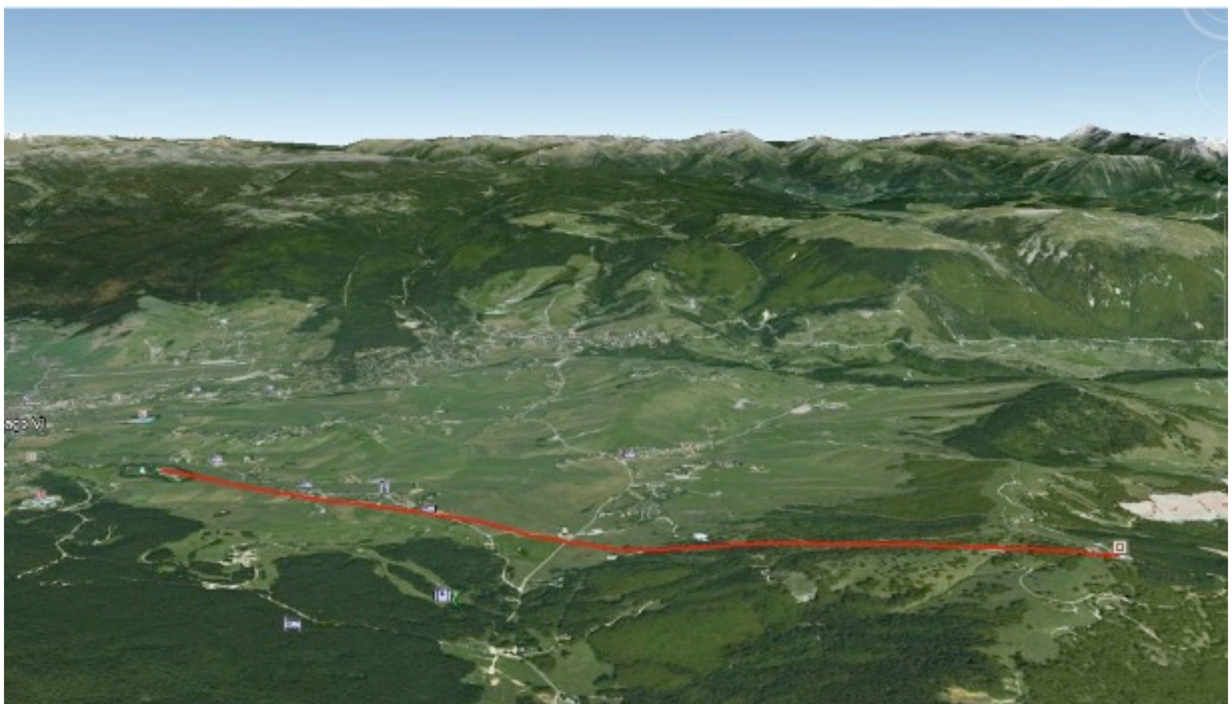

The two main observing facilities in Asiago, the 1.2 m Galileo telescope (T122) and the 1.8 m Copernicus telescope (T182), located in Pennar and Cima Ekar respectively.

Preliminary results with Aqueye+

A preliminary test has been already performed, namely the measurement of the correlation between the four sub-apertures of the 1.8m telescope with Aqueye+, essentially **at zero baseline. The blue star Deneb (surface temperature 8500 K) was used.** We could obtain two sets of data**:**

Obs. 1: **Hα** filter (λ = 656.3 nm), $\Delta\lambda$= 3.0 nm

Obs. 2: **OIII** filter (λ = 500.7) nm 1800 s, $\Delta\lambda$ = 1.5 nm

However, the measured $\mathbf{g^{(2)}}$ was in both cases 5-10% **smaller** than 1. This result is possibly caused by some systematic loss of coincidences in the acquisition chain. To verify such explanation, we computed the ratio of measurements performed between the same channel pairs with the two filters. This ratio turns out to be 1, in line with expectations.
Narrower optical filters (0.3 nm) have been acquired in the meantime, and observations will be repeated as soon as possible.

Observations using both telescopes have also been made, their analysis is still in progress.

Intensity Interferometry with future optical telescopes and with Cherenkov Light telescopes

Futuristic: SII with VLT + ELT?

As already shown, Cerro Paranal and Cerro Armazones are 22km apart, in an almost E-W configuration, **not in direct view, but for SII not important.**
The rotation of the Earth will perform the synthesis, pushing the angular scale by 100x from VLTI (200m).

2020? ELT: full Quantum Astronomy

Not obvious which stellar sources could be the best target fo a 22 km baseline. Spots on stellar surfaces? Studies are needed

The MAGIC Cherenkov light telescopes on the Roque

Feasibility of optical SII with the MAGIC telescopes - 1

MAGIC potentials for intensity interferometry (even in moonlight conditions)

- The largest currently operating stereo system, with two *large telescopes of 17 m diameter*
- Parabolic mirrors with active mirror control can be used to improve focusing to infinity and ensure isochronicity at the focal plane
- a photomultiplier (PMT) for optical observations is present at the focal plane in the central pixel of the camera. The signal from the PMT is transmitted through an optical fiber to an acquisition room, where it is digitized and stored for analysis

What else is needed?

- *Narrow band filters* in front of the central PMT with a module to reduce the effects of central wavelength shifts due to different inclinations of the beam
- A *split pupil* would allow measurements of the correlation at zero baseline, that would extend significantly the spatial coverage of the degree of coherence
- *Fast acquisition system* capable to store the time of arrival of the photons with sub-ns relative accuracy for hours (might already be there)

Disadvantage: Single baseline of 80-90 m

Scarce coverage of the u-v plane, no image synthesis possible, but non negligible E-W component, hence baseline component perpendicular to the incoming wavefront changes during the night

Feasibility of optical SII with the MAGIC telescopes - 2

With the above mentioned additions, MAGIC would be able to *resolve stars and their environments with sub –milli-arcsec resolution.*

For a maximum sustainable rate of 60 Mcounts/s, measurements ***with 1% accuracy*** are possible for stars brighter than V=2.5 mag

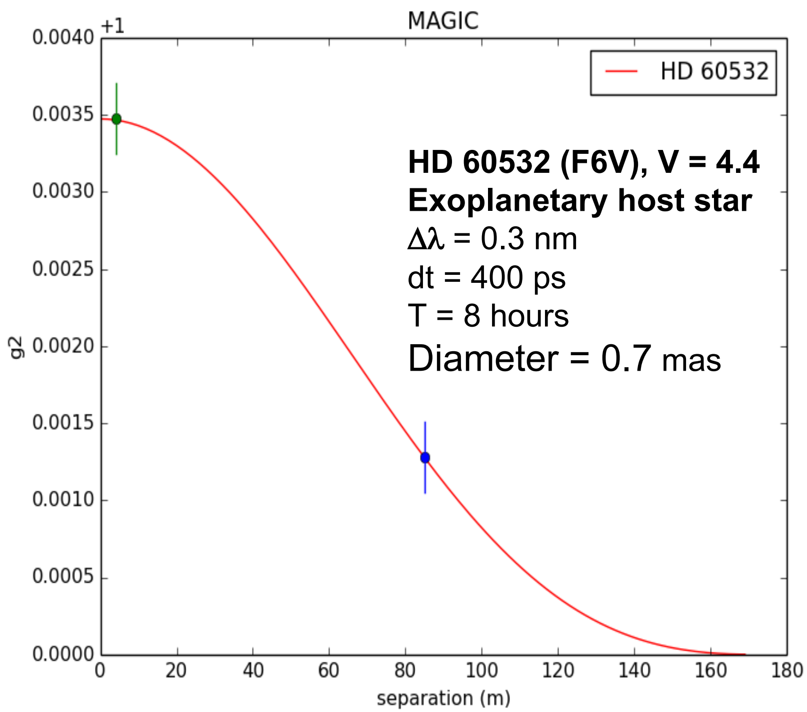

A simulation of what can be achieved

Prospects for optical SII with CTA

The Cherenkov Telescope Array (CTA) can be considered as a non-gamma-ray-astronomy device for SII

The N telescope of CTA shall provide both large photon fluxes and N(N-1) baselines, making thus possible ***image reconstruction*** thanks to the good coverage of the (u-v) plane.

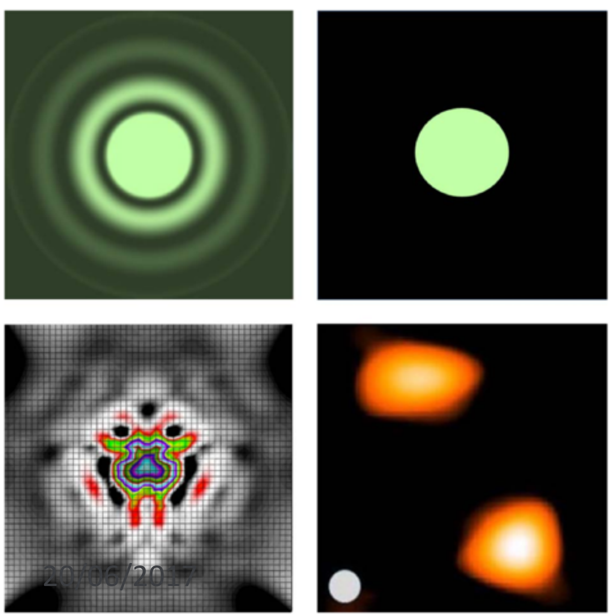

Lund experiment (Dravins 2016)
Simulated telescopes with SPAD detectors and 180 baselines on optical bench.
Intensities between pairs were correlated at 10 MHz, providing a good coverage of the Fourier u-v plane (left)
Optical image of an asymmetric binary (bottom right) was reconstructed

The ASTRI prototype

Prototype for CTA Small Size Telescope with Schwarzschild-Couder configuration (4.3m primary, 1.8m secondary, strongly aspheric mirrors, aplanatic, PSF 9.9 arcminutes, high isochronicity ≈ 3 **ps). SII could be performed with an Astri array.**

Some results on optical pulsars

What are pulsars?

Rotating neutron stars, remnants of Supernovae explosions

Solar mass, Diameters 10 km, density neutron matter

Rotational periods: from sub-milliseconds to seconds

Several thousands are known in the radio domain

Only a handful are also optical emitters, and only two (the pulsar in the Crab Nebula and Geminga) visible from both hemispheres.

Timing of the CRAB pulsar

Supernova exploded in year 1054, well visible to naked eye for months, observed by Chinese and Korean astrologers, and American natives in New Mexico

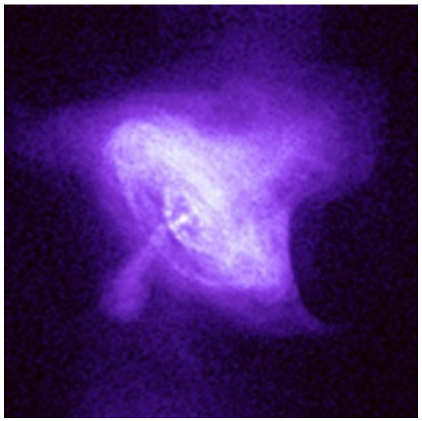

X-ray

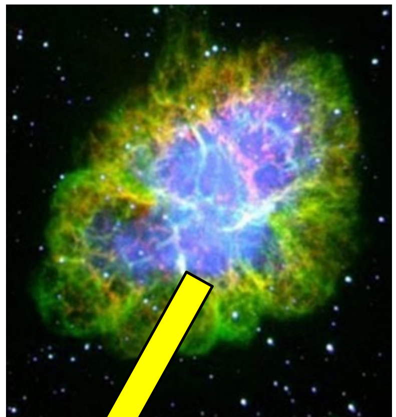

optical

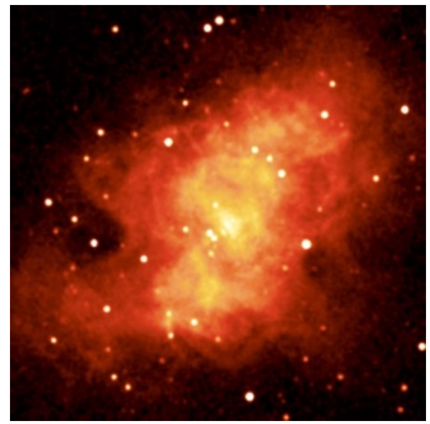

infrared

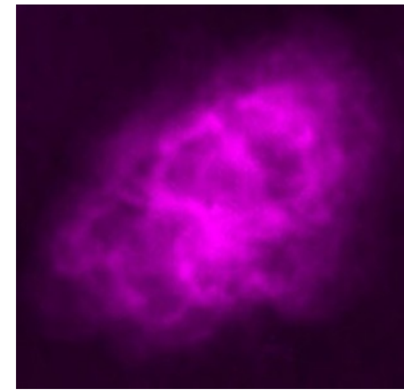

radio

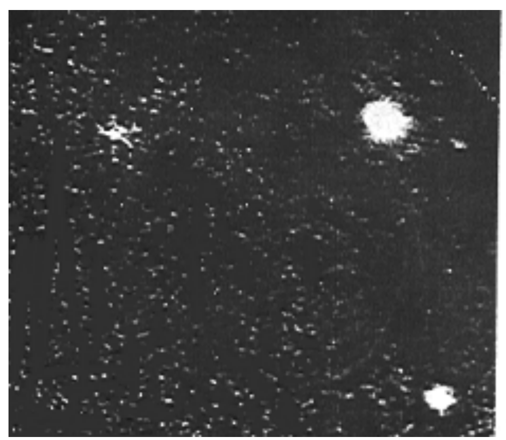

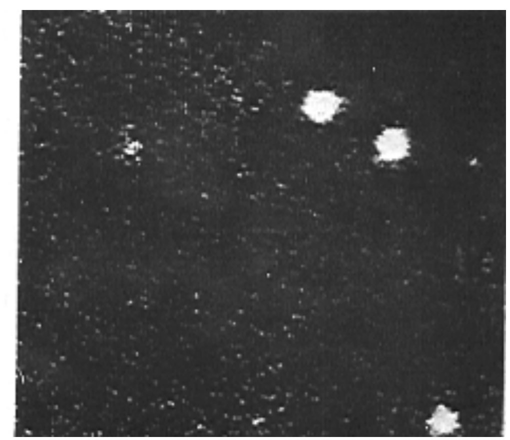

The optical pulsar in the Crab Nebula

This is the remnant of the Supernova. The pulsar period of 33 ms is slowing down at a rate of about 10^{-8} sec per day, small but enough to be detected by Aqueye and Iqueye after few hours, a complication indeed for data reduction.

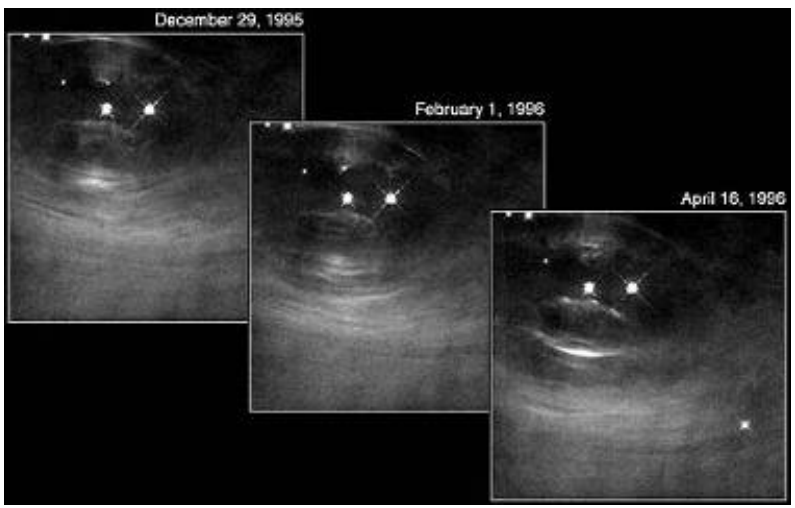

Moreover, the complex, time-varying and polarized background would require a space-resolving photometer, e.g. a CCD-type array of SPADs.

Aqueye - Two days in Oct. 2008

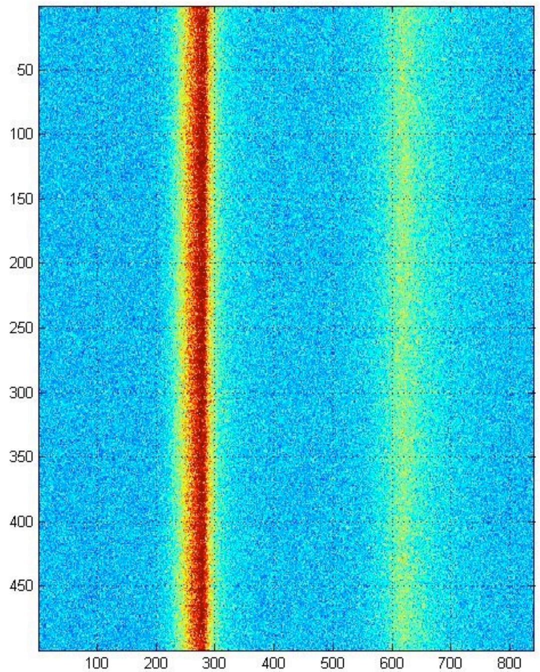

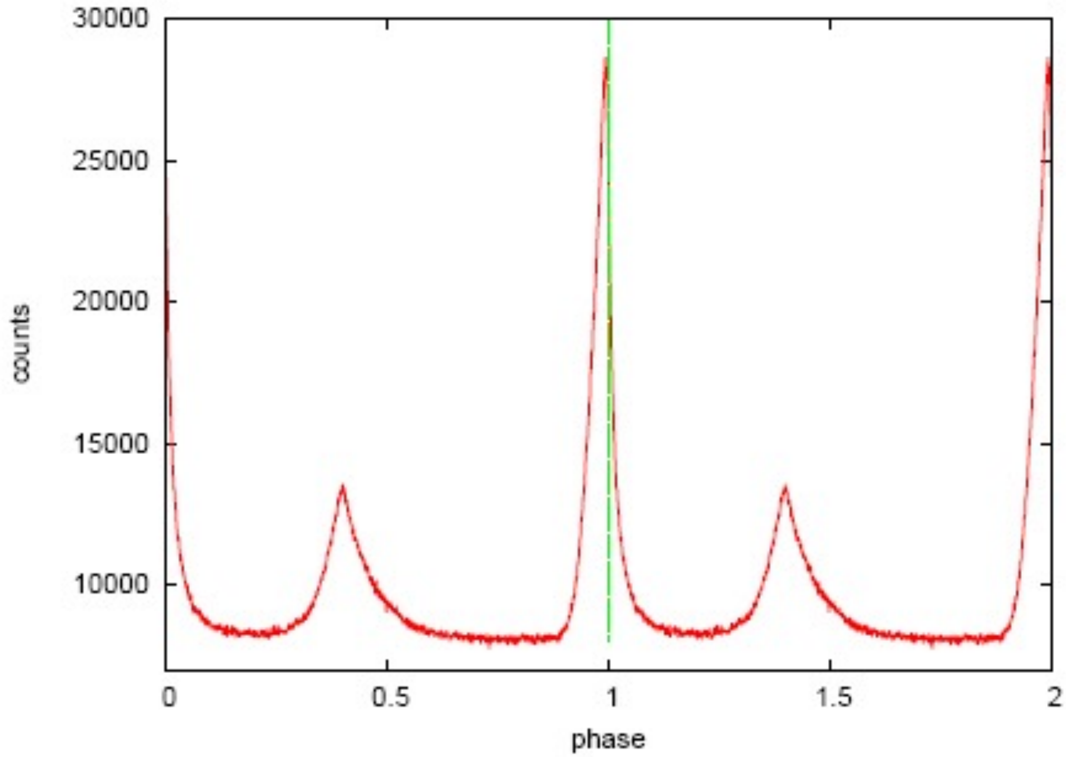

Folded light curve of the Crab pulsar. The folding period and the bin time were 0.0336216417 s and 33.6 μs, respectively. For sake of clarity, two rotations of the neutron star are shown.
Phase zero/one corresponds to the position of the ***main peak in the radio band*** and is marked with a vertical *green dashed line.*

Phase drift and phase residuals

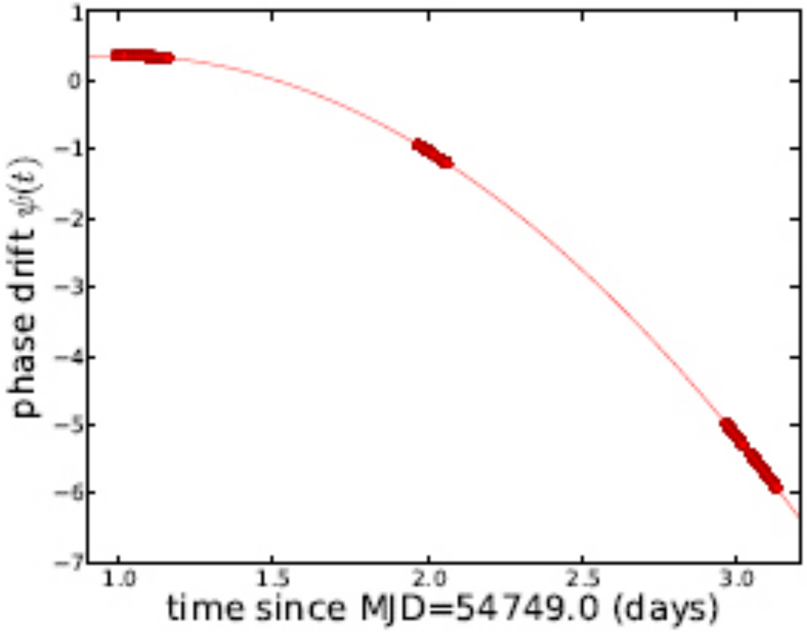

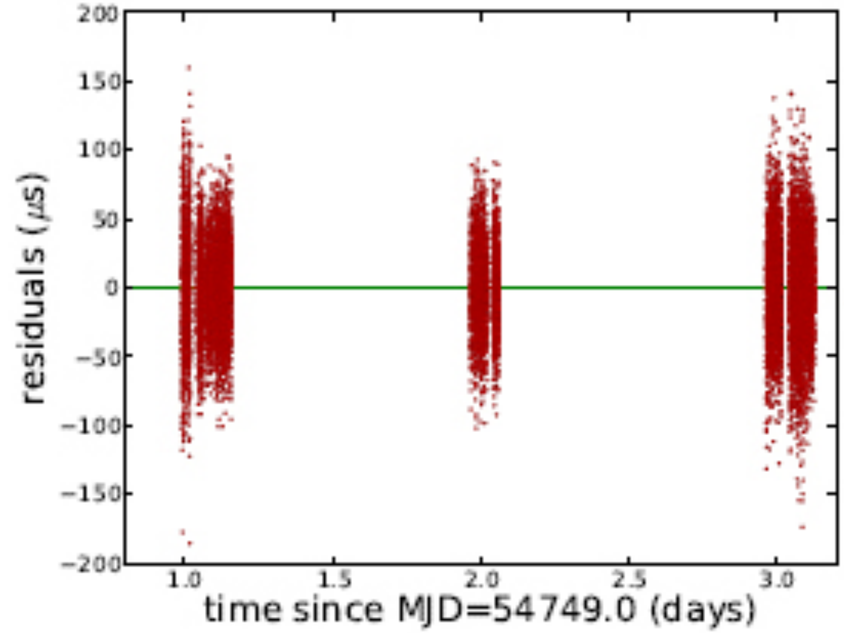

Left panel: Phase-drift of the main peak of the Crab pulsar measured during the observing run in Asiago in October 2008. The red curve is the best-fitting parabola. The reference epoch t_0 is *MJD=54749.0,* while the reference rotational period is P_{init} = *0.0336216386529 s.*

Right panel: Phase residuals (in μs) after subtracting the best-fitting parabola to the phase-drift, showing the existence of a **phase noise**.

Iqueye at the NTT - 2009

The Crab pulsar was observed at the NTT in Chile in January 2009 and again in December 2009.

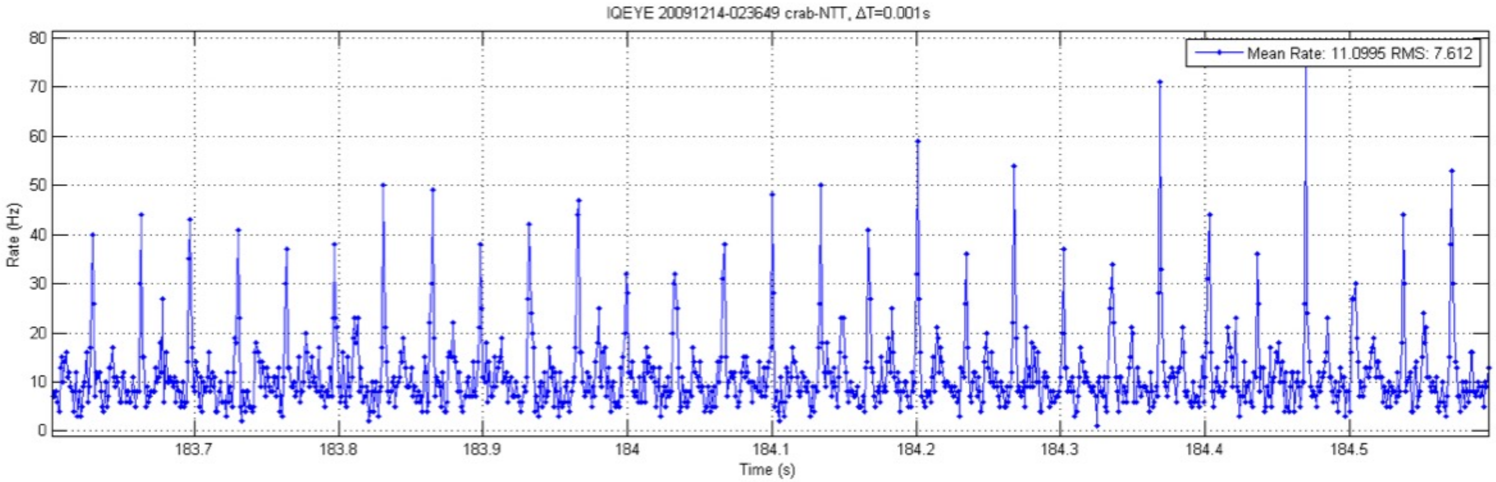

Thanks to the higher photon flux with respect to the 1.8m telescope, individual primary and secondary pulses could be detected. The LC was already very good after 30s of integration, with a time bin of 0.1 microseconds.

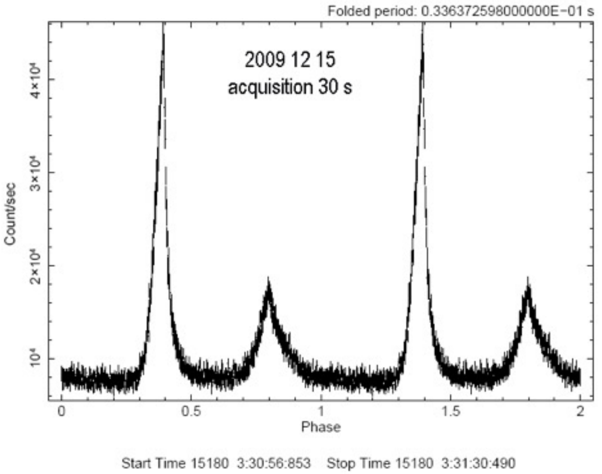

Optical - radio phase difference

s
te
th
M
al
b
if

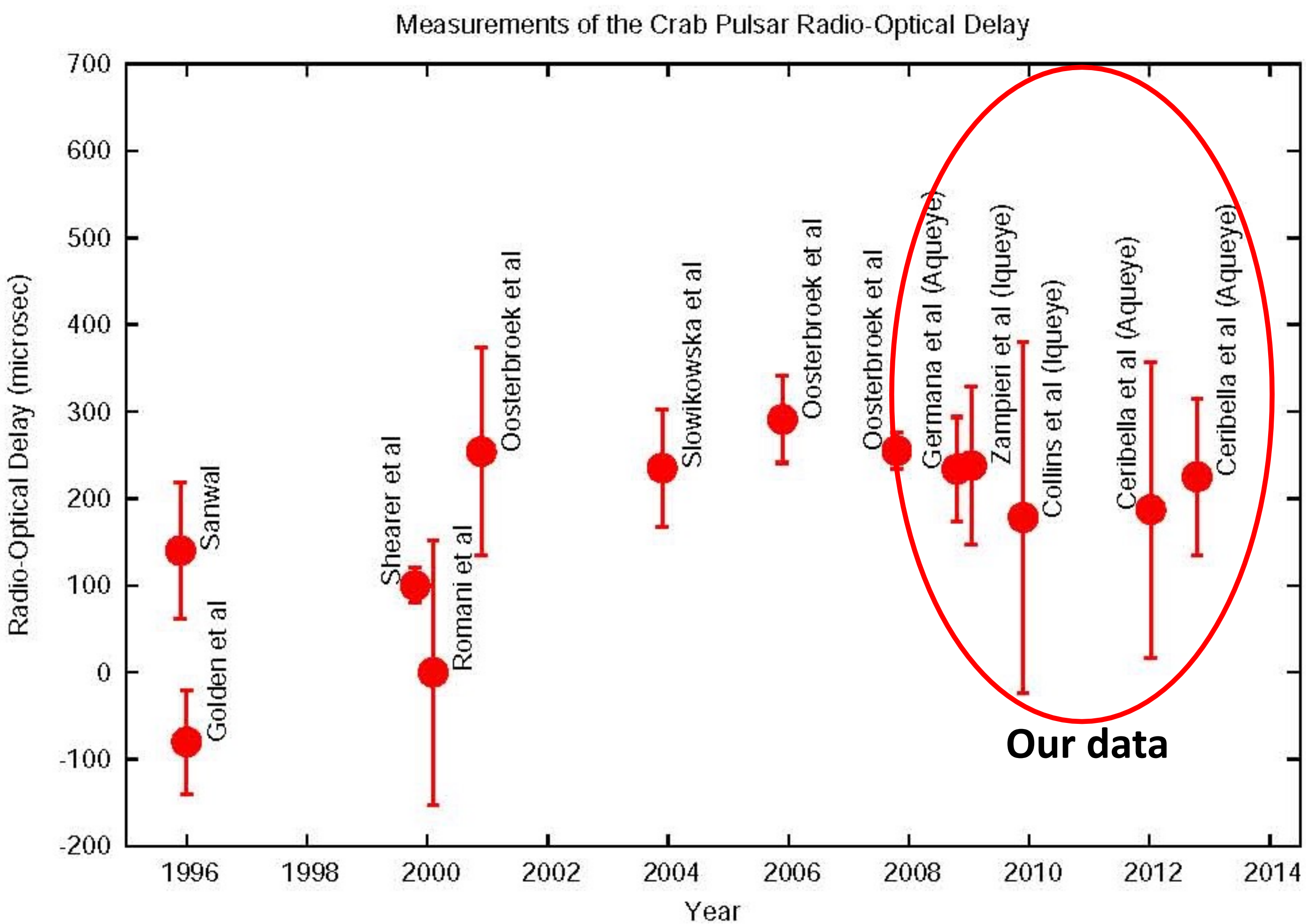

Phase residuals

After removing the radio-optical delay in arrival time of the primary peak, phase differences are within ***20 microseconds*** or so (less than 1/1000 rotation).

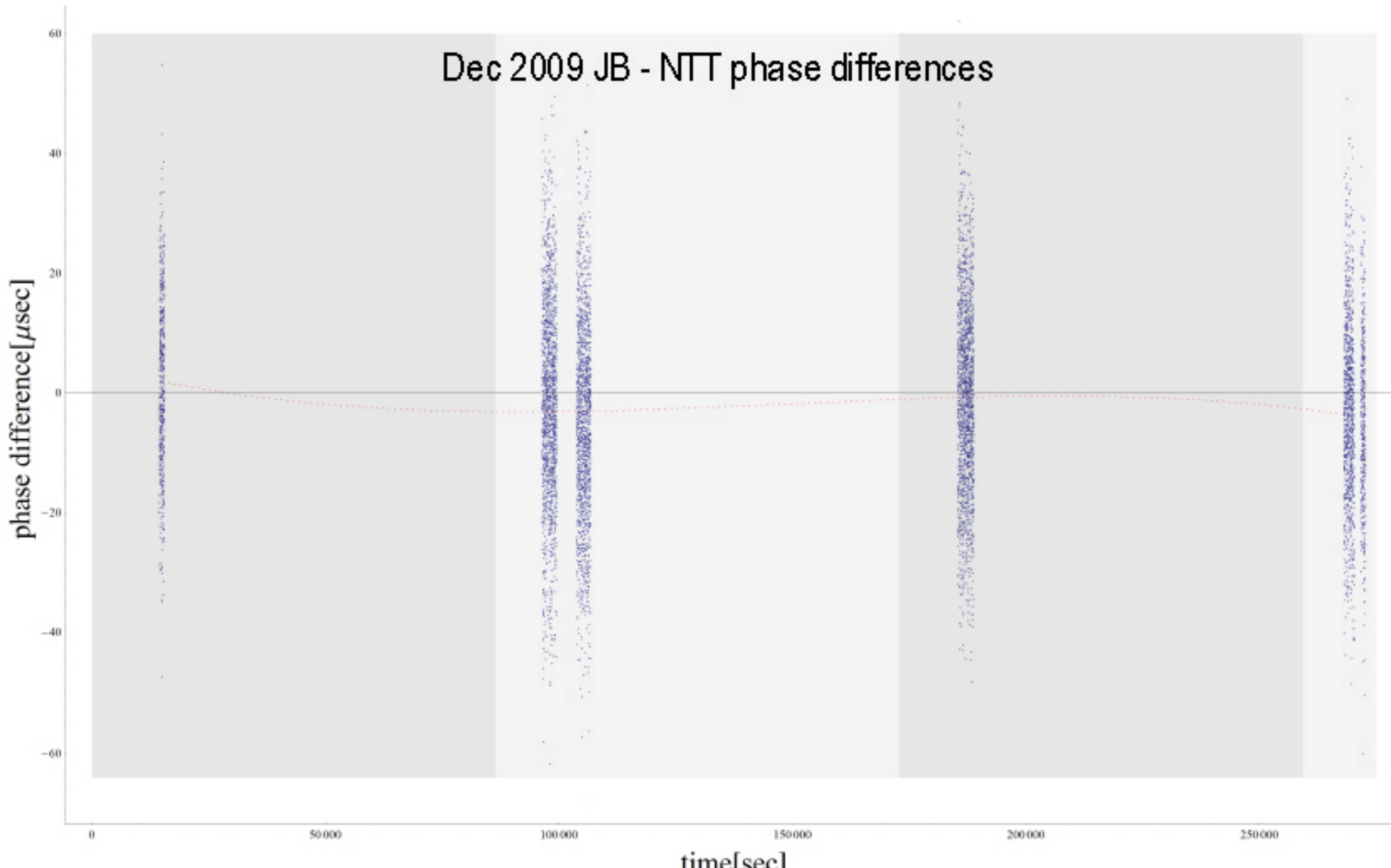

Optical signature of Giant Radio Pulses - 1

The concurrent Jodrell Bank **radio** observations were de-dispersed, cleaned and analyzed to find so-called '**Giant Radio Pulses**' (GRPs), occasionally emitted with an intensity 1000 times higher than that of a typical pulse. **737 GRPs** were identified by JB above a 6.0-σ cutoff, and out of them, **663 had concurrent optical observations**.

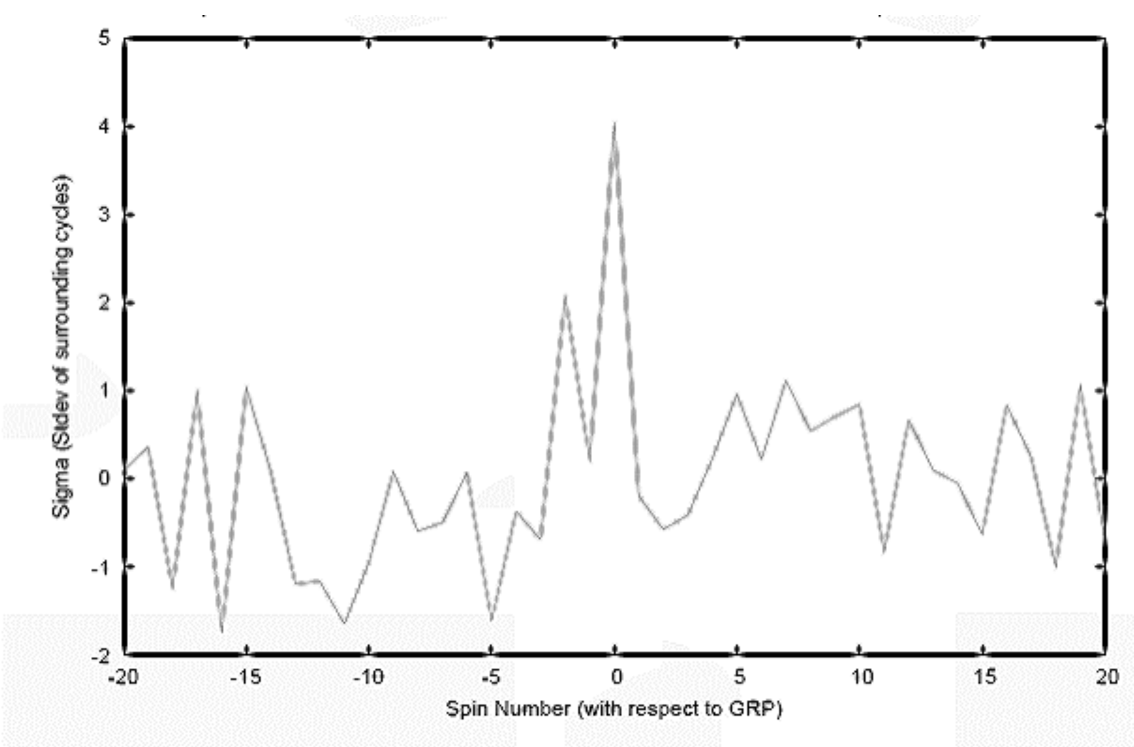

The plot shows ***a noticeable increase in optical flux*** up to a 4-σ level in correspondence with the radio GRP, in agreement with previous findings (Shearer *et al., 2003)*

The second brightest pulsar: B0540-69 in the Large Magellanic Cloud

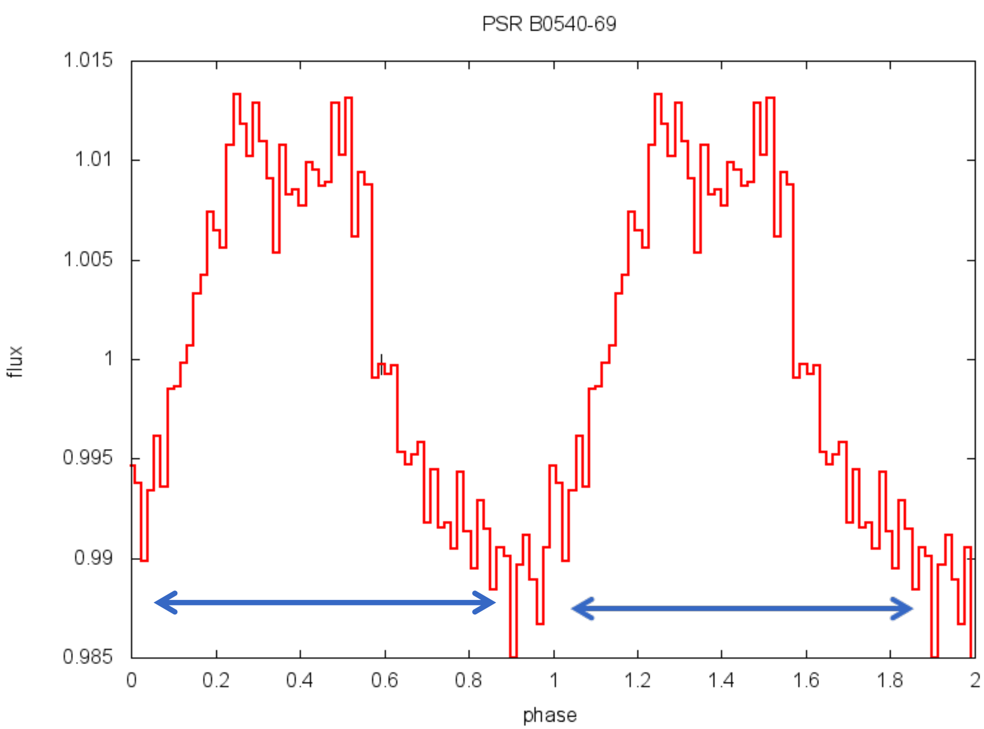

Two cycles are shown for clarity. The double peak structure is plainly visible, but there is a suspicion of an even more complex shape.

This pulsar is approximately 100 time fainter than Crab's, therefore individual pulses could not be detected. We extended by 9 years the time span over which optical data have been obtained and derived **the best light curve.** The braking index over 27 years of observations is ***n*** **= 2.087 +/- 0.013,** decidedly lower than the magnetic dipole value n=3**.**

2015 - The Fermi LAT detection

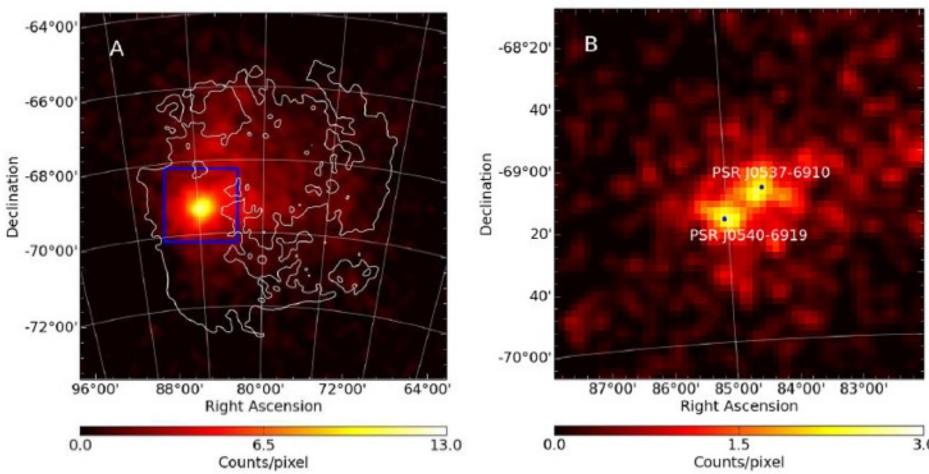

Figure 1: **Sky maps of the LMC.** (A) 0.2–200 GeV gamma-ray emission in a $10° \times 10°$ region encompassing the LMC. The map was smoothed using a Gaussian kernel with $\sigma = 0.2°$. Emission is strongest around 30 Doradus (approximately delimited by the blue box), but also fills much of the galaxy. Contours show the atomic gas distribution. (B) 2–200 GeV gamma-ray emission in a $2° \times 2°$ region around 30 Doradus. The map was smoothed using a Gaussian kernel with $\sigma = 0.1°$. Better angular resolution at higher energies resolves two components coincident with PSR J0540−6919 and PSR J0537−6910, whose locations are indicated as blue dots. Both maps are given in J2000 equatorial coordinates.

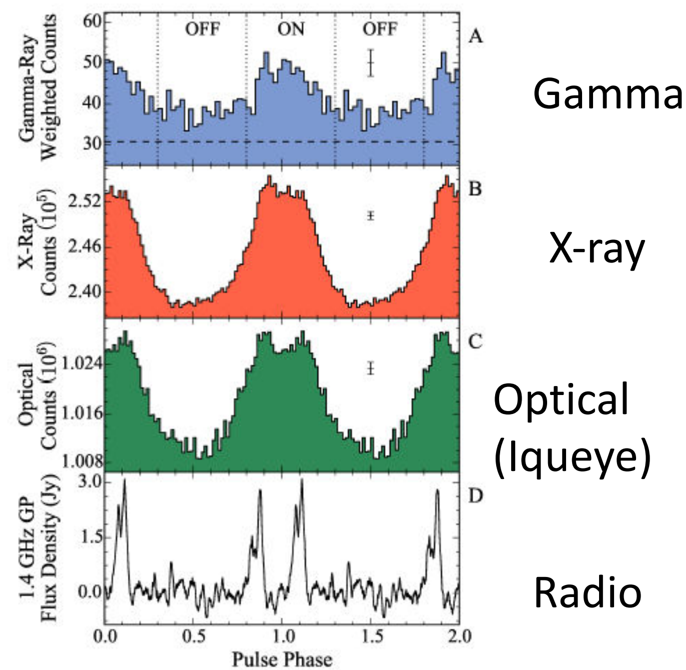

Excellent agreement of the light-curve shape from Gamma to optical. Notice the superior quality of the Iqueye data.

Figure 2: **Pulse profiles for PSR J0540−6919.** (A) Probability-weighted LAT count profile. The horizontal dashed line approximates the background level. Vertical lines indicate the on- and off-pulse regions used for the LAT spectral analysis. (B) RXTE X-ray integrated count profile. (C) NTT optical count profile. (D) Parkes radio flux profile from summing 18 bright giant radio pulses at 1.4 GHz. Two complete cycles are shown. The error bars in the top three panels represent the median phase bin errors.

The faintest pulsar: Vela

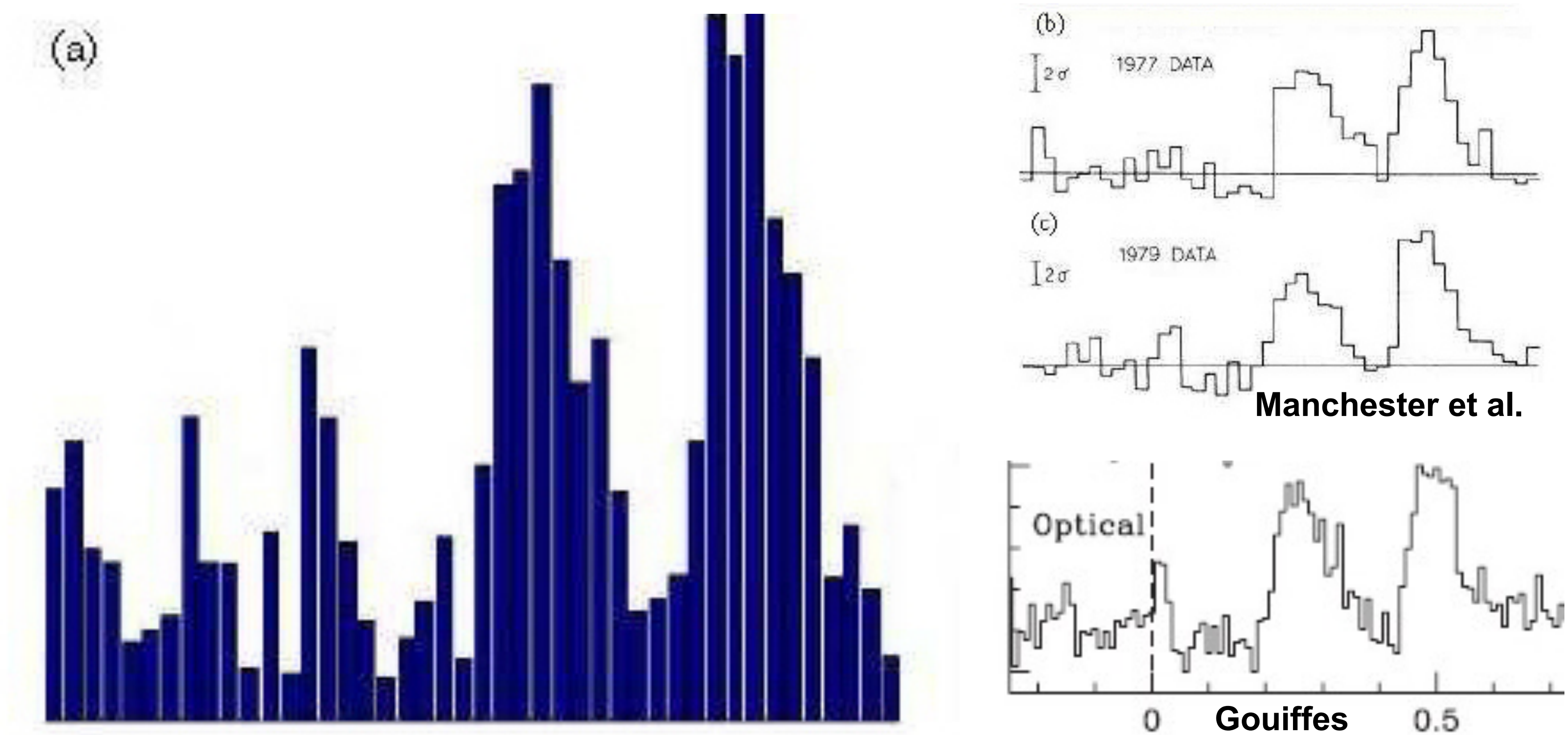

Vela's pulsar (period around 80 ms) is 10 times fainter than B0540-69.

The light curve (1 cycle shown here), again the best in the literature, has ***a very complex shape***.

Few references

Čadež A; Zampieri L; Barbieri C; Calvani M; Naletto G; Barbieri M; Ponikvar D (2016) *What brakes the Crab pulsar?* Astronomy & Astrophysics Volume 587 id A99, 11 pp

Fermi LAT Collaboration; Ackermann M; Albert A; Baldini L; Ballet J; Barbiellini G; Barbieri C; Bastieri D; Bellazzini R; Bissaldi E; and 107 coauthors (2015) *An extremely bright gamma-ray pulsar in the Large Magellanic Cloud* Science Volume 350 Issue 6262 pp 801-805 (2015)

Fermi LAT Collaboration; Ackermann M; Albert A; Baldini L; Ballet J; Barbiellini G; Barbieri C; Bastieri D; Bellazzini R; Bissaldi E; and 107 coauthors (2015) *An extremely bright gamma-ray pulsar in the Large Magellanic Cloud* Science Volume 350 Issue 6262 pp 801-805 (2015)

Zampieri, L.; Verroi, E.; Barbieri, M.; Naletto, G.; Barbieri, C. (2015) *High-time-resolution observations of supernovae with Aqueye+: ASASSN-14kg, PSN J07285597+5611462, PSN J09204691-0803340*, The Astronomer's Telegram, No.6875, **Bibliographic Code: 2015ATel.6875....1Z**

Zampieri L; Čadež A; Barbieri C; Naletto G; Calvani M; Barbieri M; Verroi E; Zoccarato P; Occhipinti T (2014) *Optical phase coherent timing of the Crab nebula pulsar with Iqueye at the ESO New Technology Telescope*, Monthly Notices of the Royal Astronomical Society, Volume 439, Issue 3, p.2813-2821, **DOI: 10.1093/mnras/stu136 Bibliographic Code: 2014MNRAS.439.2813Z**

Barbieri C, Naletto G, Verroi E, Zaccariotto M (2013**)** *Aqueye Plus: a fast photometer with an optical vortex coronagraph*, 6 September 2013, SPIE Newsroom. **DOI: 10.1117/2.1201308.005043**

References -2

Zampieri L; Verroi E; Naletto G; Mignani, R; Sigismondi C; Barbieri C (2013) *Optical Observations of the Crab pulsar from March 2 through 4, 2013, with Aqueye at the Copernico telescope in Asiago (Cima Ekar Observatory),* The Astronomer's Telegram, #4878 , 02/2013

Shearer A; Collins S; Naletto G; Barbieri C; Zampieri L; Germana C; Gradari S; Verroi E; Stappers B (2013) *High-Time-Resolution Optical Observations of the Crab Pulsar,* Electromagnetic Radiation from Pulsars and Magnetars. Proceedings of a Conference held at University of Zielona Góra, Zielona Góra, Poland, 24-27 April 2012. San Francisco: Astronomical Society of the Pacific, p.11

Germanà C; Zampieri L; Barbieri C; Naletto G; Čadež A; Calvani M; Barbieri M; Capraro I; Di Paola A; Facchinetti C; Occhipinti, T.; Possenti, A.; Ponikvar, D.; Verroi, E.; Zoccarato, P. (2012) *Aqueye optical observations of the Crab Nebula pulsar*, Astronomy & Astrophysics, Volume 548, id.A47, 7 pp,

Collins S; Shearer A; Stappers B; Barbieri C; Naletto G; Zampieri L; Verroi E; Gradari S (2012) *Crab Pulsar: Enhanced Optical Emission During Giant Radio Pulses*, New Horizons in Time-Domain Astronomy, Proceedings of the International Astronomical Union, IAU Symposium, Volume 285, p. 296-298

Barbieri C; Naletto G; Zampieri L; Verroi E; Gradari S; Collins S; Shearer A (2012) *Aqueye and Iqueye, Very-High-Time-Resolution Photon-Counting Photometers*, New Horizons in Time-Domain Astronomy, Proceedings of the International Astronomical Union, IAU Symposium, Volume 285, p. 280-282

Thank you!